AAiT

ADDIS ABABA INSTITUTE OF TECHNOLOGY

አዲስ አበባ ቴክኖሎጂ ኢንስቲትዩት

ADDIS ABABA UNIVERSITY

አዲስ አበባ ዩኒቨርሲቲ

ADDIS ABABA UNIVERSITY

ADDIS ABABA INSTITUTE OF TECHNOLOGY

SCHOOL OF MECHANICAL AND INDUSTRIAL ENGINEERING

Design and Simulation of Solar Powered Evaporative Cooler for Storage of Tomato

A Thesis Submitted to the School Graduate Studies of Addis Ababa University in Partial Fulfillment of the Requirement for the Degree of Masters of Science in Mechanical Engineering (Thermal Engineering)

By: Seniya Fedlu Surur

Advisor: Dr. Eng. Muaz Bedru

July 4, 2024

Addis Ababa, Ethiopia

DECLARATION

I hereby confidently Declare that the work which is being presented in this MSc this entitled as "Design and simulation of solar powered evaporative cooler for Storage of Tomato".

Seniya Fedlu surur — Signature — Jun 28/24 — Date

Name

This thesis has been submitted for examination with the approval of university advisor

Dr. Muaz Bedru Hussen — Signature — July 01/2024 — Date

Advisor

ADDIS ABABA UNIVERSITY

ADDIS ABABA INSTITUTE OF TECHNOLOGY

SCHOOL OF MECHANICAL AND INDUSTRIAL ENGINEERING

Thermal system and energy conversion chair

DESIGN AND SIMULATION OF SOLAR POWERED EVAPORATIVE COOLER FOR STORAGE OF TOMATO

Submitted in accordance with the requirements for the degree of master of science (M.Sc.)

Approved by Board of Examiners

Advisor	Signature	Date
Approved by Board of Examiners		
Dr. Muaez Bedru		01/07/2024
Advisor	Signature	Date
Dr. Yilma Tadesse		28/06/24
Internal examiner	Signature	Date
Dr. Habtamu Tkubet		01/07/24
External examiner	Signature	Date
Dr. Abdulkadir Aman		01/07/24
Thermal engineering chair	Signature	Date
Dr. Araya Abera		01/07/24
Dean of smie AAit	Signature	Date
Dr. Sosina Mengistu		
Director of post graduate	Signature	Date

iii

ACKNOWLEDGEMENT

I would like to start by expressing my gratitude to Almighty **Allah** for providing me with the endurance, wisdom, and patience that I needed in order to complete my research.

My gratitude goes to my parents, who supported be financially and emotionally by being by my side through my hole work. Then my thanks go to my advisor, Dr. Muaz Bedru Hussen, who has been advising, guiding, and mentoring me in all my research steps, sharing his wealth and wisdom without holding back.

ABSTRACT

Post-harvest loss is one of the major problems that need great consideration to address challenge of food security. This issue is mostly common in Africa, especially in sub-Saharan Africa due to lack of electricity, high energy cost to income ratio and attempts to harnessing solar powered energy. However, Ethiopia is one of the high fruits and vegetables producing regions in Africa continent. But due to lack of proper storage around 20% of the harvested product gets spoiled since the region has a semi-arid climate condition which is unsuitable for storage of tomato. The safe storage temperature of tomato ranges between 18ºC to 22ºC. This temperature range can be achieved with refrigerators and evaporative coolers. However, the cost of refrigeration system is very high compared to evaporative coolers and they also consume large amount of electric power for the same cooling effect. Thus, considering that there is no electrical coverage in the farming areas, a solar powered evaporative cooler would be more suitable for storage of tomato in the region. A direct evaporative cooler with a capacity of 100kg is designed and its performance is studied with simulation on ANSYS Fluent. The effect of varying the thickness of the cooling pad, inlet velocity and inlet temperature on the performance of the cooler is studied. Three pad thicknesses (50mm, 75mm and 100mm), inlet velocities of (0.5m/s, 1m/s, 1.5m/s, 2m/s and 2.5m/s) and inlet temperatures (25℃, 27℃, 29℃ and 33℃) are considered. The result shows that larger pad thickness has a higher temperature drop at the outlet compared to the pad with smaller thickness. The cooling capacity and cooling effectiveness also increases as the thickness of the pad increases because increasing the thickness of the pad increases the heat transfer area. Increasing the velocity of the air at the inlet increases the outlet temperature. Increasing the inlet velocity also increases the cooling capacity and cooling effectiveness since increasing the velocity increases the flow of air which favors the heat transfer. Optimum cooling conditions for tomato storage are achieved at larger thickness of the pad (100mm) and 0.5m/s inlet velocity.

Key words: Solar powered evaporative cooler, Cooling capacity, Effectiveness, ANSYS Fluent

Table of Contents

LIST of FIGURES

LIST of TABLES

LIST OF ABBREVIATIONS

A	Ampere	w	Humidity Ratio
AC	Alternative Current	V	Voltage
ACD	Air Change per Day	Whr	Watt hour
DC	Direct Current	WBT	Wet Bulb Temperature
DBT	Dry Bulb Temperature	$\in$	Emissivity
DPT	Dew Point Temperature	CFCs	Chloro Fluoro Carbons
Eff	Equipment Efficiency	CFD	Computational Fluid Dynamics
FUM	Motor Use Factor	TR	Tons of Refrigeration
PV	Photovoltaic	TPH	Tons per hour
RH	Relative Humidity	RH	Relative Humidity
RHS	Rectangular hollow sheet	HVAC	Heating, Ventilation and Air Conditioning

LIST OF SYMBOLS

ACL	Air change load (W)	Ti	Indoor ambient temperature (K)
Cp	Specific heat capacity (kJ/kgK)	To	Outdoor ambient temperature (K)
I	Current (A)	Tw	Wet bulb temperature (K)
k	Thermal conductivity (W/m.K)	U	Over all heat transfer coefficient (w/m^2^{o}C)
M	Mass of the product (kg)	V	Volume of cold storage (m^3)
Ma	Mass of air (kg)	V	Voltage (v)
Mw	Mass of water vapor (kg)	ε	Direct evaporation effectiveness (%)
P	Horse power rating (w)	A	Area
Q	Heat transfer rate (w)	l	Characteristic length (m)
R	Heat flow resistance (m^2 ^{o}C/W)		

CHAPTER ONE

1. INTRODUCTION

1.1. Background of the study

The horticulture sector plays a vital role in supporting human nutrition and as an income generation for people in various parts of the world (Verploegen et al., 2019). And the demand is increasing yearly with increase in population. However, postharvest losses currently are expected to be around 20–50% and in developing countries, these losses may exceed half of the actual agricultural product (Mahmood et al., 2019). Like many developing countries, the majority of Ethiopia's population is engaged in farming and about 80% the countries food products are cultivated by small farmers. However, these farmers do not use proper postharvest management technologies and most of the products are lost after production and before reaching the market. The hot and humid climate prevailing in most developing countries and the lack of infrastructure plays a vital role for such enormous losses (Ayele, 2018b). Such losses not only deprive the private societies, but also optimize substantial waste of resources employed during its production. This in turn affects the food security and market stability of a nation by creating large inflation in food products (Basediya et al., 2011).

The quality of fruits and vegetables and their associated shelf life are reduced by loss of moisture, decay and physiological breakdown. These deteriorations are directly related to storage temperature, relative humidity, air circulation, mechanical damage, and improper postharvest sanitation. But the major post-harvest losses occur due to storage of products in unfavorable ambient air temperature and humidity (Kesavan, 2018). Therefore, management of temperature and humidity is crucial for extending the storage life of the harvested product with high quality. In developing countries, postharvest fruits and vegetables are lost due to lack of storage facilities. Vegetables and fruits also known as perishable crops; if not preserved quickly as soon as harvested, they shrivel, whither or rot away rapidly, especially under hot condition (ADEBISI, 2015). Fruits and vegetables need to be stored at lower temperature since they are perishable in nature. Nearly 35% of all fresh products, in developing countries like Ethiopia, are lost due to lack of cold storage facilities and absence of regular power supply (Samue, 2013).

The cultivated tomato (*Lycopersicon esculuntum Mill*) is the most important and widely grown vegetable in the world with a production of 186.82 million of metric tons in 2020, worldwide (Branthôme, 2022). Production of tomato in Ethiopia has shown a marked increase and it became the most profitable crop providing a higher income to small scale farmers. During the 2016/2017 cropping season, the total annual tomato production was estimated to be 283,648.27 quintals (Putter et al., 2012). Kombolcha is one of the regions in Ethiopia known for its high production of vegetables. It produces around 6,120 quintals of tomato yearly. But due to its semi-arid climate condition around 20% of the production gets spoiled due to improper storage (Tegegn, 2013). And the lack of electricity coverage in the area has made proper storage of products very difficult. Thus, post-harvest deterioration of tomatoes is very frequent for kombolcha.

Researches show that lowering the temperature of a tomato to an appropriate level slows down the deterioration and thus increases the length of time the tomatoes can be stored. Currently, control of temperature and humidity of a system can be achieved using evaporative coolers, refrigeration system and dehumidifiers. But the latter two require high electrical power and uses expensive parts for their construction are inappropriate for the needs of the local farmers, who incidentally produce the bulk of fruits and vegetables. These make their investment, running and maintenance cost more expensive than evaporative coolers (Zakari M. D et al., 2016). The result of researches done to date demonstrates that evaporative cooling can reduce temperatures below ambient with a depression reaching 12°C and relative humidity above 90% and thus showing potential for preservation of fresh produce (Tolesa & Workneh, 2017). However, studies have revealed that conventional electric-powered cooling systems could not be of much use in rural areas of Africa because of non-availability of energy sources (Basediya et al., 2011). Therefore, alternative low-cost cooling systems need to be sought. According to researches, Ethiopia has a good solar energy potential in most of its regions. The daily average radiation of Ethiopia is considered to be 5.26kWh/m^2 on yearly basis. Therefore, a solar powered evaporative cooler can be used since solar energy is cheap and readily available (Tesema & Bekele, 2015).

Therefore, the focus of this study ensures the use of a low-cost solar powered evaporative cooling system with less energy demand in the preservation of fresh tomato products for extended periods in their marketable state.

1.2. Evaporative coolers

Evaporative cooling is the process by which the temperature of a substance is reduced due to the cooling effect from the evaporation of water. The conversion of sensible heat to latent heat causes a decrease in the ambient temperature as water evaporated provide useful cooling. This cooling effect has been used on various scales from small space cooling to large industrial applications. Evaporation of water produces a considerable cooling effect and the faster the evaporation the greater is the cooling (Basediya et al., 2011; Shahzad, 2019). Evaporative coolers can be classified into, direct evaporative coolers (DEC), indirect evaporative coolers (IEC) and combined IEC/DEC. DEC are the simplest types of evaporative coolers in which the inlet air and water are brought into direct contact and the cooling occurs when sensible heat of the water is converted into latent heat. In IEC, the air first passes through the heat exchanger as opposed to passing straight to the humidifier as is the case with direct EC. In combined IEC/DEC or two stage systems, IEC is often paired with a second direct evaporative cooling stage to cool the supply air further while adding some moisture to the supply air (Chaudhari et al., 2015; Lizcano et al., 2020).

1.3. Statement of problem

The challenge of post-harvest losses of highly perishable fruits and vegetables in Ethiopia, such as potatoes, tomatoes, carrots, peppers, and mangoes. While communities with access to electricity can use refrigeration for storage, rural farmers lack the technology to preserve their produce, leading to significant spoilage and economic losses. This situation not only impacts producers but also poses health risks to consumers. Our main focus to design and simulate a cooling storage solution, specifically for tomatoes, this is due to changeable electricity supply and high temperatures, there is significant spoilage of these perishable items, which results in economic losses and food insecurity. The use of a solar-powered evaporative cooler is proposed as a suitable and energy-efficient option for these areas. Our issue to solve focuses on evaluating the performance of an evaporative cooler through simulation using ANSYS software, with the goal of providing a design and sustainable solution for the storage of tomatoes and other perishable agricultural products in rural areas of Ethiopia.

The research seems to advocate for the use of inexhaustible energy solutions to address these problems, specifically focusing on the design, simulation, and performance evaluation of a solar-powered cold storage facility for tomatoes, which are particularly vulnerable to spoilage.

1.4. Objectives

1.4.1. General objective

The main objective of this research is to design, simulate and study the performance of an evaporative cooler for tomato storage.

1.4.2. Specific objectives

The specific objectives of this thesis are:

- Design an evaporative cooler for storage of tomato.
- Select fan, pump, battery and solar panel for the system.
- Simulate the designed cold evaporative cooler using ANSYS Fluent.
- Study the performance of the evaporative cooler by varying operating conditions and validate the result.

1.5. Significance of the study

Cold storage is one way of protecting the deterioration of agricultural products like fruits and vegetables using evaporative cooling technology. The purpose of this study is to design solar based cold storage which operates by cooling air in order to increases the shelf life of the perishable agricultural products. Designing of an evaporative cooler using solar PV panel energy source creates a proper storage of perishable agricultural products for areas with no coverage of electricity. Thus, the research aims to benefit farmers, merchants, and investors and consumers in the kombolcha, which is a city known for its high production of perishable agricultural products, especially tomato.

1.6. Scope and Limitation of the Study

This research covers design and geometrical modelling of the cooling units for the case of Kombolcha atmospheric conditions, and the numerical simulation is performed using ANSYS Fluent. The performance of the cooler is studied using the simulation result by varying the thickness of the cooling pad and velocity of the cooling air. However, this study is limited to design and simulation of the cold storage system. Experimental test could not conduct due to budget limitation.

1.7. Organization of the study

The structure of the research is organized as follows: chapter one discusses about the introduction of the research which includes background of the research, problem statement, objective of the research significance, scope and limitation of the research. Chapter two discusses reviews of different researches in this area. Chapter three discusses about the methodology followed to achieve the objectives of the research and data used while chapter four shows the design of the solar powered evaporative cooler for storage of tomato. The simulation procedure is included in chapter five and the result and discussions are included in chapter six. The research is concluded and recommendations for future work are presented in chapter seven.

CHAPTER TWO

2. LITERATURE REVIEW

Post-harvest loss is the series issue especially in developing countries to solve and secure their food. Despite of their high production of fruits and vegetables; developing countries suffer the spoilage when they store fruits and vegetables. The loss is occurred due to lack of infrastructure like transportation, storage and power. The arrival of new technologies to simplify our daily life has been increasing and it demands energy for more expansion. Preserving foods, especially fruits and vegetables which are early perishable after harvested within few days also requires new technology with sufficient energy for users to secure their needs. To preserve these perishable foods, several studies have been conducted by different scholars at different time and conditions.

Evaporative cooling occurs when air, that is not too humid, passes over a wet surface; the faster the rate of evaporation the greater the cooling. The efficiency of an evaporative cooler depends on the humidity of the surrounding air. Very dry air can absorb a lot of moisture so greater cooling occurs. In the extreme case of air that is totally saturated with water, no evaporation can take place and no cooling occurs. Generally, an evaporative cooler is made of a porous material that is fed with water. When ambient air drawn over the material; the water evaporates into the air raising its humidity and at the same time reducing the temperature of the air. There are many different designs of an evaporative cooler. The design will depend on the materials available and the user's requirements. Evaporative coolers are easy to construct and low cost compared to other type of coolers. Due to this a lot of researches have been conducted on make these coolers more reliable and easily accessible for people in rural areas.

2.1. Principle of evaporative cooling

Evaporative cooling is a process in which the evaporation of liquid into surrounding air cools a body in contact with. Since heat is needed to turn liquid into vapor, the body's surface is much colder when water evaporates from it (Otterbein, 1996). When water evaporating into air is taken into account, the wet bulb temperature as opposed to the air-dry bulb temperature measures the potential for evaporative cooling. The evaporative cooling effect increases with the magnitude of the temperature differential between the two (Watt, 1986). Using an air-moving system in

conjunction with the natural process of water evaporation, evaporative cooling generates a cooling environment that is efficient. The fresh and warm outside air moves through the wet porous pad thus cooling the air through water evaporation.

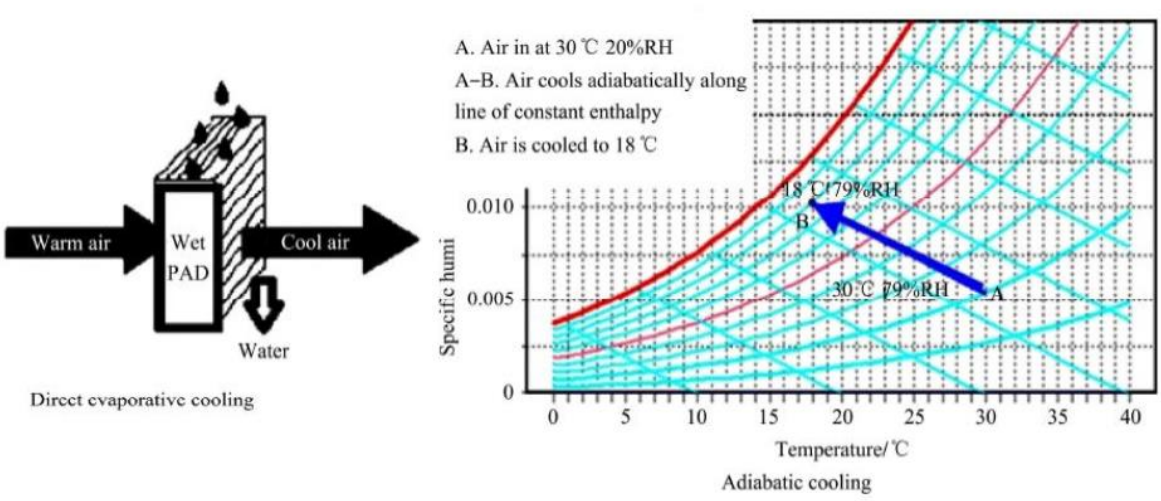

Figure 2. 1: *S*chematic of direct evaporative cooling *(*Ndukwu &Manuwa, 2014)

The evaporative cooling process is affected by the following factors.

1. **Air temperature**: When water absorbs sufficient energy to transition from a liquid to a gas, evaporation takes place. A considerable amount of water vapor may be retained in air that is rather warm, which can also encourage the evaporative process. As a result, higher temperatures will cause more cooling because of their high rate of evaporation. Lower temperatures result in less evaporation and cooling because less water vapor can be retained.
2. **Air velocity or air movement**: One significant element influencing the rate of evaporation is air movement, whether it be forced (with fans) or natural (wind). The air next to the water's surface, or the "moist area," becomes more humid when water evaporates from a wet surface. The rate of evaporation will begin to slow down as the humidity increases if the humid air remains in place. On the other hand, the rate of evaporation will either rise or stay constant if the humid air close to the water's surface is continuously being forced away and replaced by dry air.

3. **Surface Area:** the area of the evaporating surface is another important factor that affects the rate of evaporation. The greater the surface area the greater the rate of evaporation.
4. **Relative humidity of the air**: This represents the water vapor quantity found in the air as a percentage of the maximum amount the air can contain at a given temperature. Low relative humidity in the air indicates that only a tiny fraction of the total quantity of water that the air is capable of holding is being held. Since the air can absorb more moisture in this situation, a larger rate of evaporation will occur under all other favorable conditions, increasing the efficiency of the evaporative cooling system.

A research in Nigeria (Zakari M. D et al., 2016), showed that an evaporative cooler made of an aluminum wall and using a jute cooling pad was able to give a cooling efficiency of up to 83% and a temperature difference of 10ºC compared to the ambient. Total capacity of the cooler is 0.6m^3.

The same experiment was conducted by (ROLLINGS, 2019) in 2019 at the university of Makerere by only changing the capacity of the cooler. The solar evaporative coolers cooling efficiency was 82.9%, which is similar to the previous research. But the temperature difference of the cooler with the ambient air showed a reduced result which was a maximum of 7ºC. The cooler was able to store tomatoes for five days without any physical change occurring (ROLLINGS, 2019).

(Sibanda, 2019), increased the cooling efficiency of the evaporative cooler to a range lying between 86.8% and 96.7%. and the maximum temperature difference attained by the cooler compared to the ambient air is 16ºC. This research combines indirect air cooler with evaporative cooler. The research shows that the combination of evaporative cooler and indirect air cooler yields a higher cooling efficiency and a more effective cooler.

Another research which supports this concept is a (Workneh, 2020) evaluate the solar photovoltaic (SPV) system for providing cooling environment for storage of tomatoes under small scale farming which generate power run at 53 m^3 in the combined form of evaporative cooling with indirect air cooling (IAC + EC). The system was constructed from nine 330W, twelve solar modules arranged in three series and used in conjunction, 230AH Gal batteries, 5kw inverter 145VCD solar changer controller, 290W ventilation fan, 260W water pump, 3 cooling pad layer and 1760W indirect heat exchanger psychrometric unit and 3.8 tons of tomato storage chamber. The experiment was conducted by reticulating air inside the storage chamber by using solar modules, inverter, battery

and charge controller. SPV produce 2873.5W which is 98% of design power output at 80% probability exceedances and 24% higher than the required power for IAC + EC system. The tracking system under ambient conditions on daily bases has 14.9% electric power. The power output increase module temperature by 24℃ and declined thereafter. The power generated depends on the solar irradiance availability, ambient temperature and time of the day. So, the power generated during the summer season day time and excess power stored in battery could run the system until 22 hours at night when temperature lower and the system switch off.

The demand of energy in our day-to-day life increase the introduction of new technology and May not seems to slow down at any time soon. But this high energy demand adds energy depletion risk and environmental issues. Therefore, air conditioner, chiller and refrigeration have considerable amount of energy usage and provide massive environmental impacts. These technologies sound luxury, but highly needed to achieve food security. Even though solar thermal is popular technology, PV integrated refrigeration used to supply electric energy required to drive absorption cycle and compare with commercial AC absorption refrigeration system. So, the COP of AC and DC system was about 0.18 and 0.014 respectively with 10.2 years payback time (Arputham, 2021).

(Sipho Sibanda & Tilahun Seyoum Workneh, 2020)Try to identify and reduce the postharvest loss (PHL) of fruits and vegetable to improve food security for small scale farmers of sub-Saharan Africa (SSA). Farmers experiences in the production of small-scale fruits and vegetables of high PHL because of physiological deterioration which associated with biological, technical and environmental factors and also lack to access of PH facilities. According to this study the farmers experienced cooling technology which helps them to supply sufficient fresh produced to consumer by improving its nutrition and their income. But the cooling technology they have been using requires electric energy which is capital intensive and not available at small scale farmers. The review proposes as researcher carried out on solar and wind powered evaporative cooling at remote ad isolated area where no access to grid electric for hot dry and hot humid conditions.

(Ambuko & Wanjiru, 2017) Conduct the study on the effectiveness of evaporative charcoal cooler in order to preserve kales and tomatoes at outdoor condition and micro climate of cooler were investigated by measuring air temperature and relative humidity. During the study period due to light rain and low solar radiation the maximum temperature difference of inner and outer cooler and also relative humidity were 9.2℃ and 36.8 % respectively. Despite this light rain, the cooler

maximum efficiency was 91.5% which is promising shelf life and color change of tomatoes and kales.

Leafy vegetables are highly perishable and need to be consumed immediately after harvest. Unless and otherwise, it deteriorates by biological and environmental factors with temperature. So evaporative cooling using zero brick cooler (ZEBC) and evaporative charcoal cooler (ECC) preserve the quality of postharvest leafy amarathous vegetables. Freshly harvested vegetables were separated into bundle weighing of 300gram and stored under ZEBC, ECC and ambient room conditions. Temperature change, relative humidity, physical weight loss (PWL), wilting index, hue angle and vitamin C were determined by.

(Ambuko & Wanjiru, 2017)The change in temperature versus ambient air is between 4℃ to 10℃ while 80-100% relative humidity in both evaporative cooler 47.6% PWL compared to 10.5 and 6.7% under ZEBC and ECC respectively. In general, the better vegetable quality was preserved under ECC and ZEBC.

Figure 2. 2: A brick zero energy cooling chamber (ZECC) (Ambuko & Wanjiru, 2017).

Fruits and vegetables need to be stored at lower temperature because of they are highly perishable in nature. For this reason, there are many methods of cooling, preserving food in fresh from demand they control of space temperature and relative humidity by restricting their chemical, biochemical and physical changes. So evaporative cooling is the well-known system to increase shelf life of fruit and vegetables in tropical and subtropical by lowering the temperature and increasing the relative humidity (Beera, 2013).

During experimental test of fruit storage by (Vanndy, 2008) a simple brick walled evaporative cooler with Cambodia design (Lao design) and insulation for testing of mature green and breaker fruits, the temperature decrease by 1-10℃ and relative humidity increase by about 10-35%. As a result, the weight of CLN1462A and TLCV15 decrease considerably while EC had no effect on ripening except TLCV15 fruits from Cambodia experiment which is higher in decay than ambient temperature. However, decay in EC storage was 2% bicarbonate for 3 minutes in Cambodia design, it didn't vary in Lao experiment storage condition 50, CLN 1462A had lower soluble solids while lower sensor quality than TLCV15 fruits.

.

Evaporative cooling was tested and evaluated by (Muhammad, 2016) using tomato with solar powered designed and constructed systems of 0.6m^3 capacity in order to increase shelf life stored vegetable. The storage system was made up of aluminum sheet meat os 1mm thickness and the side wall made up of jute pad get moist by water flowing through perforated pipe from reservoir located at the top. The relative humidity (RH) and weight loss of tomatoes analyzed by T-test to compare with ambient condition. The cooling system has 83% efficiency by lowering temperature from ambient by 6-10℃ and increase relative humidity (RH) by 85% to preserve tomato for about 5 days while in ambient start to rotting within 3 days.

(Amjad, 2021) design and develop solar grid hybrid cold storage system for preservation of Perishables. The system inside cold chamber airflow, and temperature distribution analyzed by computational fluid dynamics (CFD). It comprises of 21.84m^3 cold storage unit with 2 tones capacity, hybrid system of 4.5kwp photovoltaic (PV) system, 5kw hybrid inventers, and 600Ah battery bank used power the system. Vapor compression refrigeration system was coupled with 3-cooling pad as thermal backup to store cooling -4 to 4 ℃ where potatoes stored at 8℃ for 3-months from May to July and tested on grid solar and hybrid modes. The solar irradiation recorded was 5-6 kwh/m^2/day and average peak power found was 4kw. In order to eliminate torque load variable frequency drive was installed with compressor and resulted in 9.3 ampere. AC with average COP of 4.6 refrigeration unit. The average energy consumed was 15kwh with the share of 4.3kwh from grid and 10.5kwh from solar, translating 30% energy consumption from grid and 70% from solar PV modules. The overall cold storage unit efficiency controlled total weight loss 7.64% and preserve quality attributes of product during storage time.

(Babaremu, 2018) design, fabricate and evaluate an active evaporative cooling system made of 0.6mm thick aluminum and 1mm thick galvanized steel internal and external wall respectively. Internal and external wall separated by polyurethane lagging materials of 25 mm; the cooler has 3-trays. The system has 2 waited distribution networked tank of each 20L capacity with 25mm diameter PVC pipe conveying water and 0.5HP pump to circulate the water from bottom to overhead. The water drips through top and drain through jute bag. So, as water drips, a suction fan swept air in motion and blows through wetted parts. As a result, evaporative cooling takes places inside the cooling chamber by controlling temperature to 23.70℃ relative to ambient temperature 29.50℃ and relative humidity (RH) to 95.6% relative to ambient conditions.

Two stage evaporative cooler which has heat exchanger and two evaporative chamber has developed by (Jain, 2007) to improve the efficiency of evaporative cooling in order to increase relative humidity (RH) and reduce temperature. TSEC reduce temperature from 8-16℃ up to wet bulb depression of ambient air and provide 90% relative humidity and its efficiency will be 1.1-1.2% over a single evaporative cooler.

(S. Sibanda & T. S. Workneh, 2020) conduct the study to investigate the effectiveness of IAC + EC in providing optimum storage of fruits and vegetables to improve their shelf-life over ambient conditions. The system is 53m^3 storage chamber to store 3.8tones of tomatoes which powered by solar energy during day and battery bank facility during night. The performance evaluated for about 28 days, the temperature lower on average 7-16℃ and relative humidity increase by 13 - 41% higher than ambient conditions.

The storage of two tomato harvested at different maturity stage was studied by (H. Getinet, 2008) under multi-layer pad evaporative cooler and ambient temperature in semi-arid eastern part of Ethiopia. The treatment composed of 2x3x2 factorial combination of variety by randomized complete block design with 3-replication. The average temperature and relative humidity difference between ambient conditions inside cooler were 15.1℃ and 54.8% respectively by reducing 5℃ dry bulb temperature and rising 18% relative humidity. The cooling efficiency of multilayer varies from 68.3 to 84%.

However, refrigeration is a key tool in success of fresh produce African small holder farmers due to financial constraints and lack of electricity supply, sophisticated cooling system is unavailable. (Kenghe, 2015) conducted the performance evaluation of low-cost silica gel-water adsorption-based cooling system refrigeration at different cooling cycle time of 30, 60 and 90 minutes with

refrigeration cycle. The test result shows cooling cycle time influence mostly reduction in temperature of storage while both increase in hot water temperature and cooling cycle time enhance cooling capacity. It also examined on the capacity of storing fresh mangoes which resulted in 3% mass loss of fruits and vegetables at inside air temperature at 15℃ and 90% relative humidity. This implies that as new technology can be adopted for fresh fruit in sub-Saharan Africa. (Timothy, 2019) conduct experimental test on red and green tomatoes collected from popular market in omu-aran town, kwara state Nigeria and green house in land mark university teaching and research farm of omu-aran, kwara state Nigeria. The two samples were stored in active evaporative cooling system for about 7 days while few samples placed in ambient environment. After 7 days, the emerging result shows the red and green tomatoes stored in cooling system loss the weight of 8.65% and 1.54% respectively while red and green tomatoes stored in ambient condition loss the weight of 47.20% and 5.14% respectively. From this, evaporative cooler has 86.01% cooling efficiency was able to optimize the shelf-life of both tomatoes.

A new zero energy cool chamber (ZECC)of low cost and energy saving was developed by (Islam, 2014)is useful for storing fruits and vegetables where an electric supply is unavailable. The system consists of two cooling systems which are solar drive adsorption refrigerator and evaporative cooling to store fruits at moderate respiration rates. Solar driven adsorption system consists of solar collector containing activated carbon as adsorbent, condenser and evaporator cools water based by evaporating methanol and adsorbing it on activated carbon and make ice. The methanol adsorbed on activated carbon desorbed by applying solar heat and ice cool storage space for a long time without the help of electricity. The evaporative cooling system cool storage space by evaporating water from wet walls containing wet filler. The combined use of 2-cooling system reduces inside temperature of new ZECC to 12.07% while outside temperature 31.5℃ to extend shelf-life of tomatoes from 7 to 23 days.

(ADEBISI, 2015) develop solar powered evaporative cooling storage system (SPECSS) to improve the shelf-life of fruits and vegetables in rural Nigeria where almost no electric power for small holder farmers. The system capacity of the system was 0.39 m^3 with suction fan of 24w and water pump 18w powered by solar panels of 182w with battery 130Ah to charge battery and maintaining system's operation. Tomatoes, carrots, mangoes and bananas were then stored in the chamber for 3-4 weeks. The temperature depression and relative humidity from ambient conditions varied from 7.8 to 15.4℃ and 44-96.8% respectively. The shelf-life of tomatoes, mangoes,

bananas and carrots inside SPECSS chamber were 21, 14, 17 and 28 respectively as against 6, 5, 5 and 8 days for ambient storage.

(Akdemir & Bal, 2020) Conduct an analysis in order to investigate the quality loss in 'Granny Smith' apple varieties in storage by setting storage temperature and relative humidity at 2℃ and 90% respectively with evaporative cooling system. From the analysis the temperature and moisture content vary throughout the storage time based on the fruits type and varieties. The quality of fruits was analyzed from 3 (top, middle and bottom) different levels monthly. The analyze result shown us as the weight loss was 0.78%, the lowest TSS value was 14.1% the lowest fruit firmness was 5.9kg, in the bottom level, and the lowest acid value was 0.67% in the top level. It was determined the highest pH value with 3.41 in the bottom level at the end of storage while the pH of the fruit at harvest was 3.25. At the end of the storage period at the highest respiratory rate in the top level 39.1mg CO2/kg

2.2. Types of Evaporative Cooling Systems

2.2.1. Direct evaporative cooling

In direct evaporative cooling, the dry bulb temperature is diminished but the wet bulb temperature stays unchanged. Water evaporates at once into the airstream, therefore lowering the air's dry-bulb while humidifying the air. The efficiency of direct cooling relies up on the pad media. A top fantastic in flexible cellulose pad can provide up to 90% efficiency while the loosely pen wood fiber pad shall end result in 50 to 60% contact efficiency.

Figure 2. 3: Direct evaporative cooling system(Deshmukh et al., 2017).

2.2.2. Indirect cooling

In indirect cooling, one circulation of air known as major air is cooled sensibly without addition of moisture and both the dry bulb and wet bulb temperatures are reduced. Indirect evaporative coolers do not increase the humidity of air but they have greater cost than direct coolers and operate at a lower efficiency. The efficiency of oblique cooling is in the range of 60-70%.

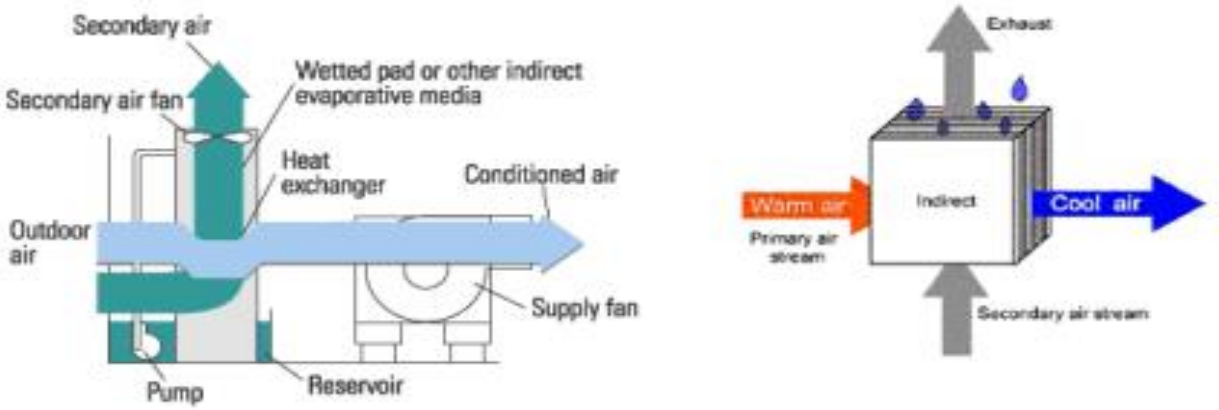

Figure 2. 4: Indirect evaporative cooling system(Deshmukh et al., 2017).

From this, we can see that direct evaporative coolers are simple by design and don't incorporate complex thermal transferring mechanism. Thus, they are low cost and smaller in size than indirect evaporative coolers (Peter Ross Enterprises, 2019).

2.3. Cooling pad material

Evaporative cooling systems consist of an exhaust fan and a pump for circulating water through a pipe positioned on top of a porous pad, figure 2.3. The fan pushes atmospheric air through the pad which is cooled by the passing water through evaporative cooling. Thus, there is transfer of heat from the pad material during evaporation and during this process water is being evaporated. The cooling ability of a machine is impartial on the quantity of air flow and its saturation which in turn relies up on the characteristics of the pad, air space through the pad and the water flow rate. Evaporation from the wetted pad is affected by wind, temperature, floor area, humidity, air velocity, saturation rate and thickness of the pad. The lower the relative humidity the higher the rate of evaporation and thus the more the cooling takes place (J.T. Libertya*, August 2013).

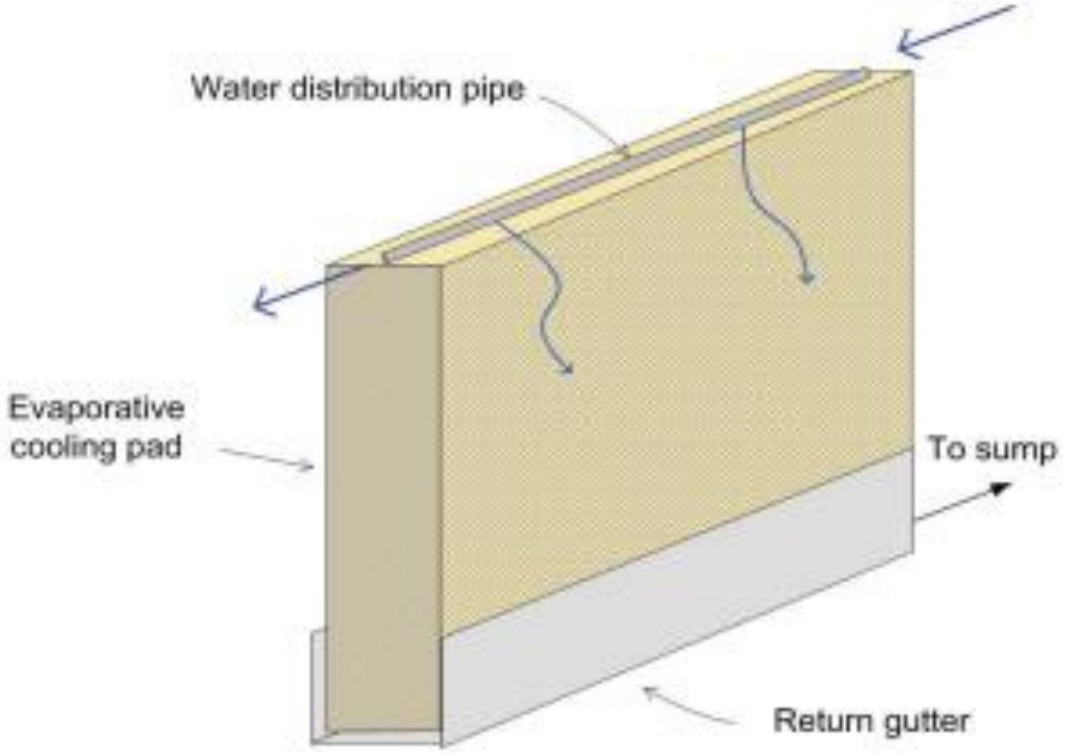

Figure 2. 5: Water circulation diagram of evaporative media pad (R. A. Bucklin, 2016).

Various materials such as palm tree leaves, hessian cloths, aspen wood, jute, cotton materials, perforated clay blocks and mad can be used as cooling pads. The material selection mainly depends on functionality, cost and availability. Easily available material includes natural fiber (its local name is Khus), which is found in many rural areas of the country. This is also used in packaging for different applications and has a high-water absorbing property for a certain time.

Figure 2. 6: Khus and its mat.

The mat made of Khus can be used to make cooling pads of different thickness by binding the mats together. Materials such as aspen fibers, palash fibers and coconut fibers are also used to make cooling pads, figure 2.5. The effectiveness of the palash fiber pad is found to be 13.2% and 26.31% more than that of aspen and khus pads, respectively. Whereas the effectiveness of coconut fiber pad was found to be 8.15% more than that of khus and comparable with that of aspen pad. Khus pad offers lowest pressure drop whereas aspen pad (most commonly used) offers highest pressure drop compared to Khus, coconut and palash pads. Palash pad is made of palash tree roots. These pads have better performance than aspen pad and Khus pads and they are easily available in most parts of the world and are low cost (J.K.Jain & D.A.Hindoliya, 2011).

Figure 2. 7: a) Aspen pad, b) palash fiber pad and c) coconut fiber.

Olosunde et al. (2009) carried out a study to test three materials (cotton waste, jute and hessian) to be used as a pad in an active evaporative cooler. The results showed that the cooling efficiency was highest for jute. The pad area depends on the cooling load required inside the cooler and the free space area of the pad. The pad free space area can be found from experimental data and the cooling load is found from the evaporative cooler design.

2.4. Insulation materials

Insulation materials are very basic and important in evaporative cooling system as it lowers the cooling load of the cooler by reducing the heat transfer between the cold storage and the ambient air (atmospheric air). The key properties of an insulating material are compressive strength, service temperature range, thermal conductivity, and water absorption and thickness tolerance. The compressive power of most insulating substances decreases as temperature increases and consequently it is critical to consider the compressive power at the service temperature. The provider temperature is the very temperature at which the insulation fabric can perform reliably in long-term application. Thermal conductivity (K) is the most important parameter in determining a material's ability to resist the flow of heat. The absorption of water in insulating cloth will increases conductivity of the cloth and motives swelling of the material. Thickness tolerance is vital for achieving alignments and product quality. A low value of thermal enlargement at running temperatures is required for the insulation (Ayele, 2018b).

In order to limit the heat received via the partition via conduction, the R-value has to be optimized. However, there will be a factor where the cost of the materials no longer justifies the additional good points in R-value. Additionally, the practical requirements of the cold storage design need to be taken into consideration (Kraemer et al., 2015).

Insulating materials fiberglass, stainless steel sheet metal, and aluminum sheet metal are analyzed for their thermal insulation property. Fiberglass has a very high thermal resistance at a low cost. Aluminum sheet metal is cheap and also good insulator especially for convective heat transfer and stainless-steel sheet metal is chipper than aluminum. Table 2.1 shows thermal insulation property of these materials (IIT Kharagpur, 2008)

Table 2. 1: Thermo-physical properties of some common constructing and insulating materials (IIT Kharagpur, 2008).

Insulating Materials	**Specific heat KJ/Kg.K**	**Density Kg/m^3**	**Thermal conductivity W/m.K**
Mineral or glass wool	0.67	24 -64	0.038
Fiberglass	0.7	64 – 144	0.04
Cork board	1.884	104-128	0.038
Cork granulated	1.88	45-120	0.045
Thermocouple (EPS)	-	30	0.037
Stainless steel	-	-	19
Steel Carbon 1%	-	-	43
Aluminum	-	-	205

2.5. Summary of literature review

As we have discussed above, many researchers have been conducted on evaporative coolers to preserve perishable commodities. The reviewed literatures include different types of evaporative coolers like direct, indirect and two stage coolers and their application, type and properties of cooling pad materials and insulation materials used for these coolers. The final results of the literature review are summarized in table 2.2.

Table 2. 2: The summary of most recent research work on evaporative cooling

No.	Evaporative cooler type	Cover material	Pad material	Cooling efficiency	Storage capacity	Reference
1	Two stage coolers	Aluminum			0.39m^3	(Kenghe, 2015)
2	Direct	Aluminum	Jute	83%	0.6m^3	(Zakari M. D et al., 2016)
3	Direct	Aluminum		91.5%		Ambuko& Wanjiru, (2017)
4	In Direct	Aluminum		86.8%-96.7%		(Sibanda2019)
5	Direct	Steel	Jute	78.4%-82.9%	0.216 m^3	(Rolling, 2019)
6	Direct	Aluminum				(Akdanye, 2019)
7	Indirect	Aluminum		98%-80%	53m^3	(Workneh, 2020)
8	Direct	Aluminum			21.84m^3	(Amjad, 2021)
9	Direct	Aluminum			20m^3	(Babaremu, 2018)
10	Direct	Aluminum		81%	35m^3	(Sibanda, 2020)
11	Direct	Aluminum		88%		(Vanndy, 2008)
12	Active evaporative cooling	Aluminum		86.01%		(Timothy, 2019)
13	Direct	Aluminum	multi-layer	68.3 to 84%.		(H. Getinet, 2008)

The literature review shows that many researchers have been conducted to increase the efficiency of the evaporative cooler for storage of perishable products. This was done by experimenting on deferent cooling pad materials, by adjusting the flow of the fan, by increasing the size of the cooling pad and through other methods. Same of the researches include experimental investigations. But there is no research done on the effect of varying the thickness of the cooling pad and the velocity of the cooling air to find on optimum performance stage for the evaporative cooler. The Research use Ansys Software to simulate the final out came and cheek the effect of varying performance like velocity of the air and thickness of the cooling pad on the performance of the system. Therefore, this research focuses on studying the effects of thickness of the cooling pad and the velocity of the air on the performance of the evaporative cooler with ANSYS numerical simulation.

CHAPTER THREE

3. METHODOLOGY

This chapter presents the methodology used to achieve the objectives of the research, data sources and collection techniques and the materials used for the research. A direct type evaporative cooler for tomato storage is designed and its performance is studied with simulation.

3.1 Data collection

Data collection and analysis are divided into two types. These are Primary data and Secondary data. Basic design data gives information about location of plants, production capacity, atmospheric condition around cold storage plants, product temperature and the loading rate. Data regarding the product which is to be stored inside the cold storage include dry bulb temperature and relative humidity that has to maintain inside the cold and maximum storage period storage inside the cold storage.

3.1.1 Primary Data

The production rate of tomato in Kombucha and the time it takes for the product to be purchased by the consumer is collected and on average a farmer needs to store around 100kg of tomato for 15 days during cultivation season.

The atmospheric conditions of Kombolcha are collected from Ethiopian National Meteorology Agency (NMA) to estimate the daily solar radiation, temperature and relative humidity of the city. Figure 3.1 shows average hourly variation of ambient temperature and figure 3.2 shows monthly average relative humidity of Kombolcha for ten years (2011 to 2020). Figure 3.3 shows monthly average solar intensity of Kombolcha for ten years (2011 to 2020).

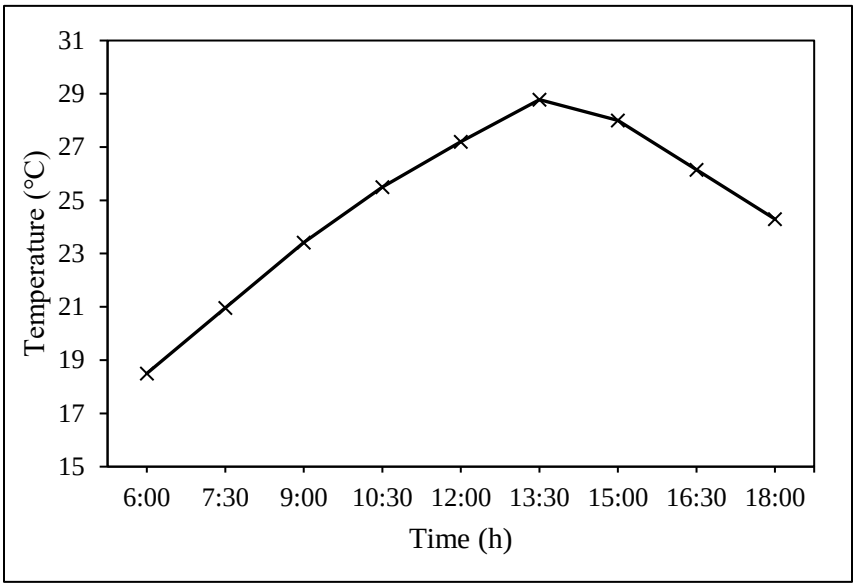

Figure 3.4: Average temperature variation of Kombolcha for average five years

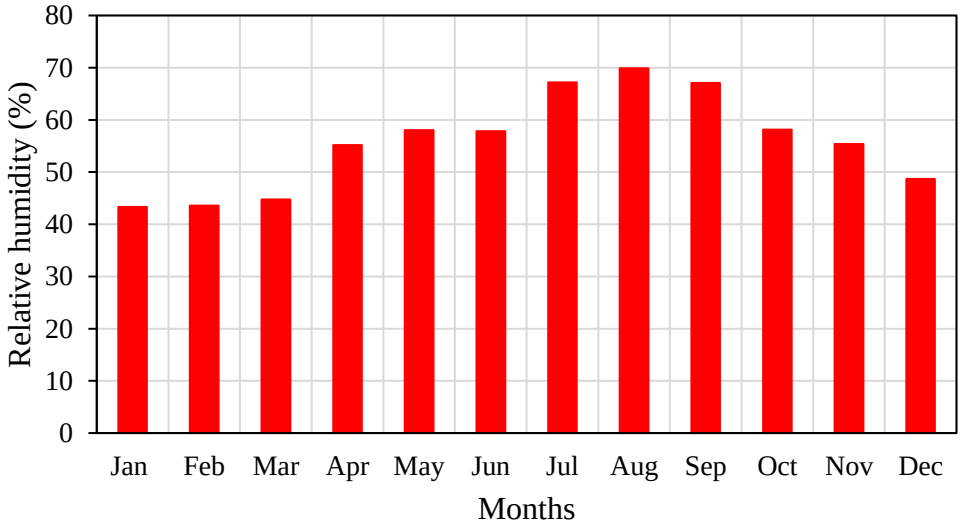

Figure 3.4: Relative humidity of Kombolcha for average 5 years.

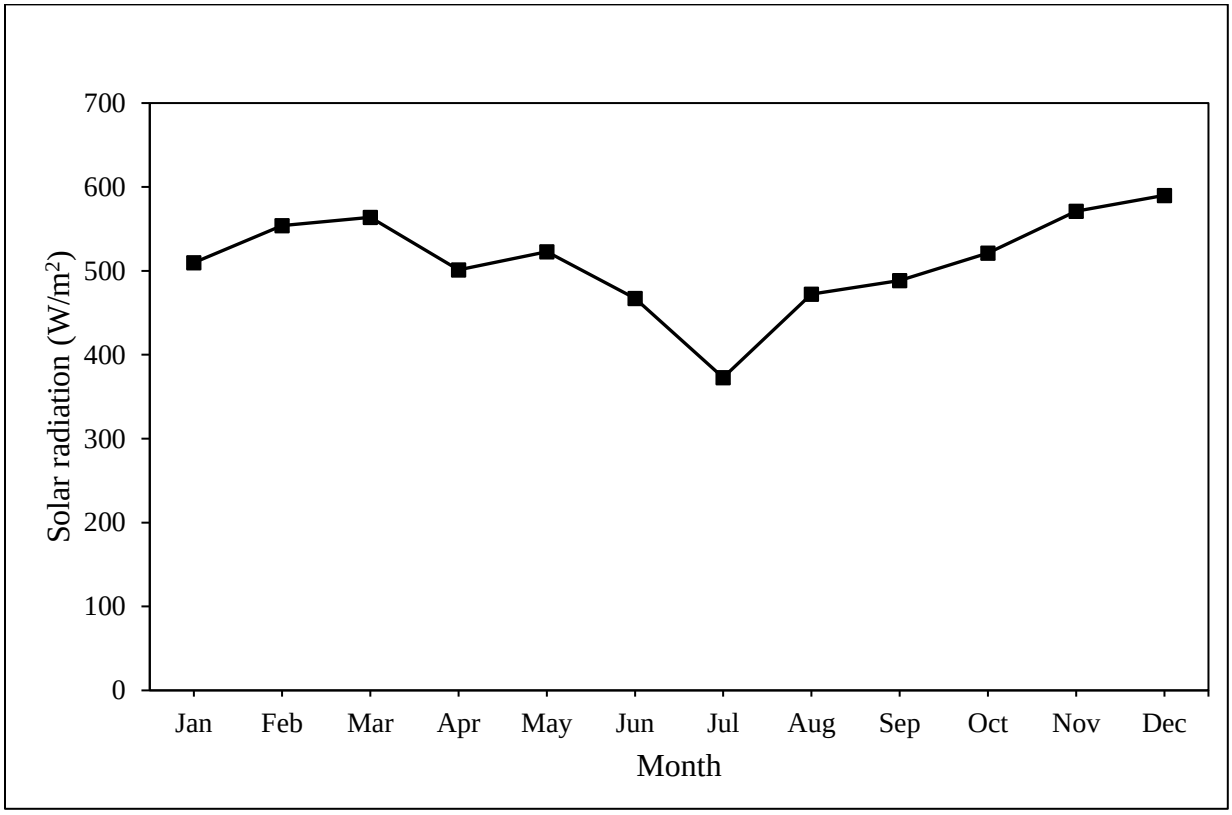

Figure 3. 1: Monthly average global solar radiation of Kombolcha.

The monthly average hourly global radiation on a horizontal surface can be determined from the monthly average daily global radiation (Duffie and Beckman, 2013) as shown in Figure 3.4.

$$\frac{I_G}{H_G} = \frac{\pi}{24}(a_2 + b_2\cos\omega)\left(\frac{\cos\omega - \cos\omega_{sr}}{\sin\omega_{sr} - \frac{\pi}{180}\omega_{sr}\cos\omega_{sr}}\right) \quad (3.1)$$

$$a_2 = 0.409 + 0.5016\sin(\omega_{sr} - 60) \quad (3.2)$$

$$b_2 = 0.6609 - 0.4767\sin(\omega_{sr} - 60) \quad (3.3)$$

Where, I_G is the monthly average hourly global radiation

H_G is the monthly average global solar radiation

ω is hour angle = [solar time – 12:00] (in hours) x 15°

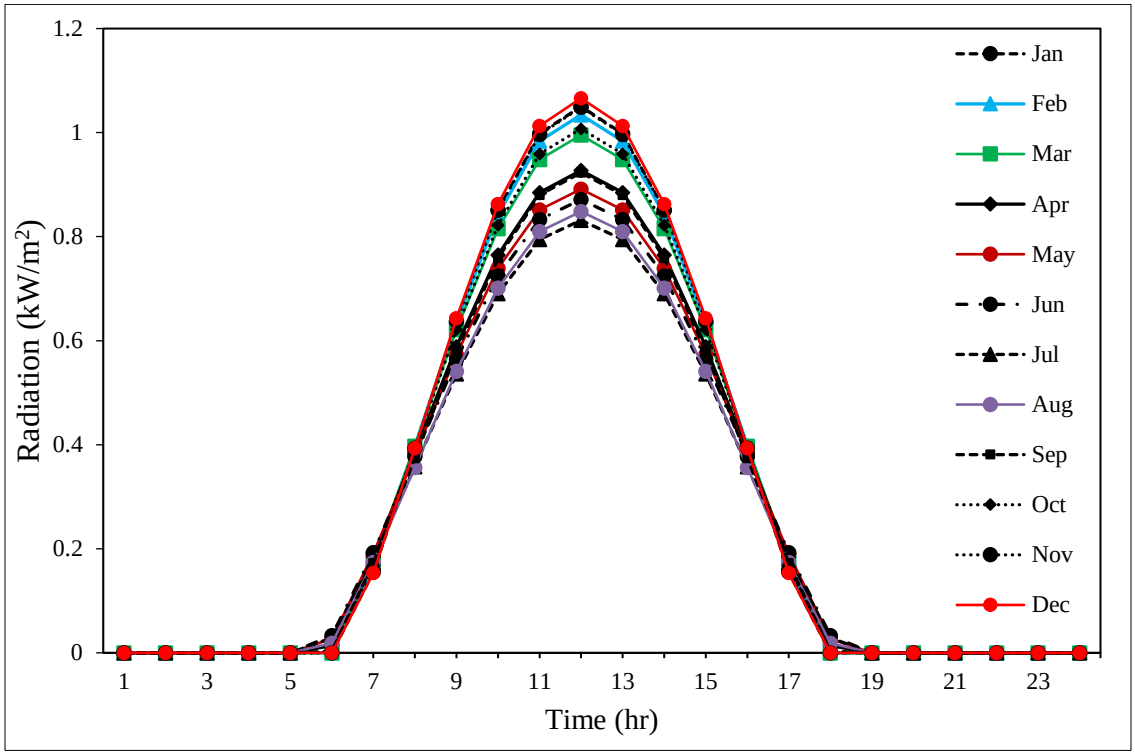

Figure 3. 2: Monthly average hourly global radiation on a horizontal surface.

3.1.2 Commodity storage requirements data

Safe storage temperature, relative humidity and shelf life of different fruits and vegetables is shown in table 3.1. The cold room of evaporative coolers should be maintained at conditions that are safe for the storage of these fruits and vegetables.

Table 3. 1:Temperature, relative humidity and storage life for some fruits, vegetables.(Khan et al., 2017)

Product	Temperature (°C)	Relative Humidity (%)	Approximate Storage Life
Pepper	9-10	85-90	6-8 weeks
Avocados	13	85-90	2 weeks
Bananas, green	13-14	90-95	2 weeks
Tomatoes, mature- green	18-22	90-95	1-2 weeks
Mangoes	13	85-90	2-4 weeks
Sweet Potatoes	13-15	85-90	4-7 months
Papayas	7-13	85-90	1-3 weeks

3.2 Materials and Methods

A direct type evaporative cooler is designed for the storage of tomato and to study its performance, simulation is done using ANSYS fluent CFD software. The overall methodology followed in this research is shown in figure 3.5.

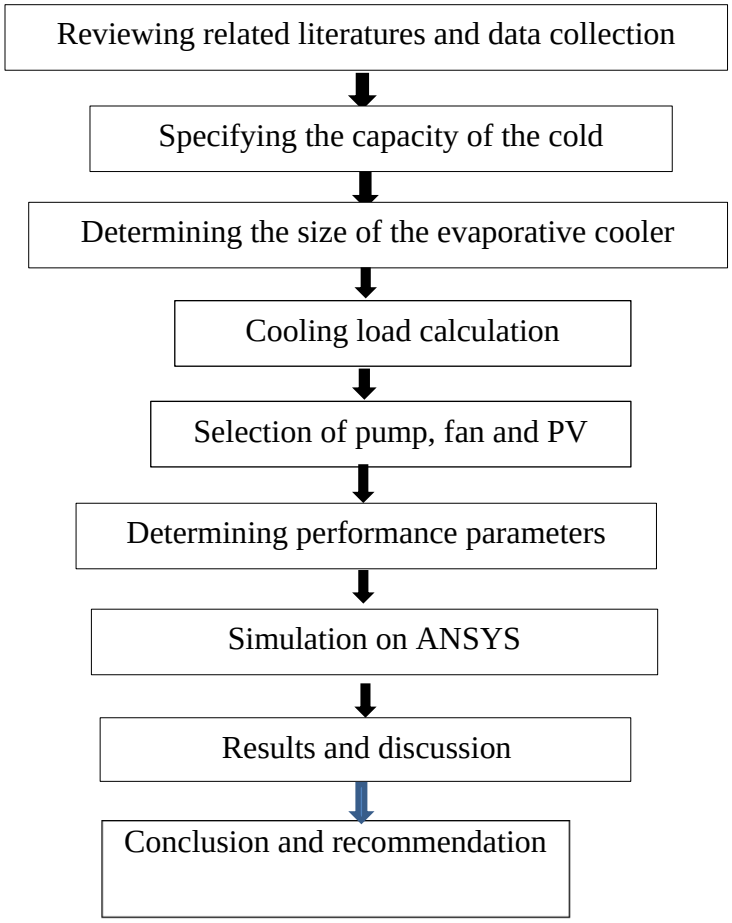

Figure 3.3: Overall methodology of the study.

CHAPTER FOUR

4. DESIGN OF THE DIRECT EVAPORATIVE COOLER

Direct evaporative coolers are simple by design and don't incorporate complex thermal transferring mechanism. Thus, they are low cost and smaller in size than indirect evaporative coolers (Peter Ross Enterprises, 2019). Direct evaporative cooling is a process in which water is evaporated and the necessary heat of vaporization is extracted from the dry air which leads to the air to be cooled. Water evaporates straight into the air stream that has to be cooled. In this process, enthalpy remains constant, the dry bulb temperature decreases and specific and relative humidity of the air increases. Direct evaporative coolers work on the principle of converting sensible heat into latent heat. Figure 4.1 shows the schematic of the direct evaporative cooler that is going to be analyzed for storage of tomato. It consists of a cooling cabinet, water pump to spray water, fan to circulate the air and a cooling pad. The air circulation is done by a fan and the pump sprays the water on the pad.

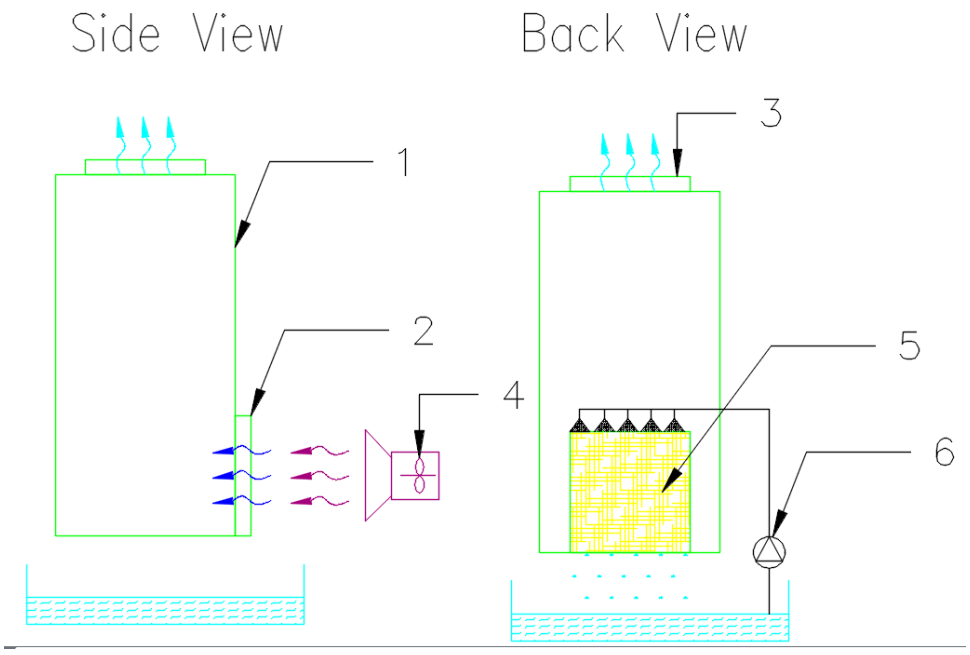

Figure 4.1: The tomato evaporative cooler

1) Cold room for tomato storage 2) Cold air inlet 3) Cold air outlet 4) Fan 5) Cooling pad 6) Water pump

4.1 Sizing the Cooling Chamber

The size of the cold chamber depends on the amount of tomato that is required to be stored inside the cooler. and this depends on production rate of tomato in Kombolcha and how much time it takes for the product to be purchased by the consumer. Thus, on average a farmer needs to store around 100kg of tomato for 15 days during cultivation season (Akdanye, 2019). The volume of cooling chamber can be calculated using equation 4.1 below.

$$width\ x\ Lengh\ x\ Effective\ Cooling\ Height = Capacity\ in\ Cubic\ meter \qquad (4.1)$$

Width x Length x Effective Cooling Height = Capacity in Cubic meter

The volume of the cooler depends on the density of tomato and the free volume required for air circulation. Increase in free volume inside the cooler will reduce the cooling time and increase the effectiveness of the cooler but at the same time it will require a larger cooler. Thus, different free volume requirement can see for different commercial coolers. Therefore, the research will consider a 60% free volume for circulation of air and loading and unloading of tomato and a 15% volume for and tomato rack(Ayele, 2020)

The volume occupied by 100kg of solid tomato can be determined from its density 970kg/ m^3 using equation 4.2.

$$\text{Volume of Tomato} = \frac{\text{Mass of Tomato}}{\text{Density of tomato}} \qquad (4.2)$$

$$\text{Volume of Tomato} = \frac{100\text{Kg}}{970\text{Kg/m}^3} = 0.10309\ \text{m}^3$$

Considering ease of loading and unloading of tomato inside the cooler, for the research purpose 0.6m x 0.6m x 1.2m length, width and height, respectively were chosen. So, the assumed free volume will be 0.6m x 0.6m x 1.2m = 0.30927 m^3**.** Thus, including the free volume assumed in addition to the volume of tomato calculated above, we will require a total volume of 0.41236 m^3. (Tasobya, 2019).

Table 4. 1: Engineering properties of some fruits and vegetables for storage (Ekpunobi et al., 2014)

Fruit and vegetable	Specific gravity	Solid density (kg/m^3)	Specific heat capacity (KJ/kg)
Lemon	1.032	1032	3.93
Tomato	1.02	970	3.67
Mango	1.068	1068	3.78
Banana	0.964	964	3.45
Carrot	0.32	320	
Orange	1.04	1040	3.91

Table 4. 2: Specifications of the Evaporative cooler(Tasobya, 2019)

Type of Commodities/to be stored	Tomato
Ventilation (Air Changes/hour)	0.5-2
Max Storage period (week) Tomato	1-3
Cold Chamber Dry bulb temperature	18-22 ℃
Cold Chamber RH	90-95%
Total Storage Capacity	100

Table 4.2: Inside cold storage condition data

4.2 Cooling Load Calculation

The air inside a cabinet receives heat from a number of sources if the temperature and humidity of the air are to be maintained at a desired level, this heat must be removed.

Cooling Load Calculation Considerations &Assumptions

Design of cooling load takes into considerations all the loads practiced by a cold storage under a specific set of expected conditions. The assumptions behind design cooling load are as follows:

- Weather conditions are selected from a long-term statistical database. The conditions will not need to represent any actual year but are representative of the location of the cold storage.

- The solar loads used are expected to be those that would occur on a clear day in the month chosen for the calculations
- The ventilation rates are either expected on air changes or based on maximum occupancy expected
- Heat flow is analyzed assuming dynamic conditions, which means that heat storage in cold storage envelope and interior materials is considered

The latent heat gain is assumed to become cooling load instantly, whereas the sensible heat gain is partially delayed depending on the characteristics of the conditioned space.

4.2.1 Heat Transmission through Walls

The conduction heat transfer through the wall or roof will depend on the thickness and thermal conductivity of the material used. In addition, there will be convection and radiation from both the back and front inside surfaces. Because of the steady state heat transfer is expressed in terms of an overall heat transfer coefficient U and the overall temperature difference between the inside and outside [$\Delta T=(T_o-T_i)$. A], wall is composite, consisting of many sections of different construction and insulating material.

Heat transfer coefficient U is the reciprocal of the total thermal resistance. The heat transfer through the cold storage building is the total amount of heat that gain through the walls, windows, ceiling, and floor of the cabinet room per unit of time (Jitendra Jayant, 2016).

$$Q_w = U \times A \times CLTD \quad (4.3)$$

Where: Q_w = heat gain through the walls of the evaporative cooler (W)

A = the outside surface area of cold storage (m^2)

U = the overall heat transfer coefficient ($W/m^2°C$)

CLTD = cooling load temperature difference (°C)

Determination of overall heat transfer coefficient (U)

$$R = R_0 + (R_1 + R_2 + \cdots R_n) \quad (4.4)$$

$$U = \frac{1}{R} \quad (4.5)$$

Where: U = The overall heat transfer coefficient ($W/m^2°C$)

R = Total thermal resistance of wall ($m^2°C/W$)

R_n = Thermal resistance through the n^{th} layer of air ($m^2°C/W$)

R_0 = Thermal resistance through the outside layer of air ($m^2°C/W$)

R_1 = Thermal resistance of layer 1 (m^2°C/W)

R_2 = Thermal resistance of layer 2 (m^2°C/W)

The cold storage walls consisting of 1 mm thick sheet metal at outer side, then 40 mm thick of fiber glass as insulation and 4 mm thick Aluminum sheet metal at inner side based on the availability. For all fronts, left side, right side and rear walls.

The total resistance from equation (4.4)

$$R = R_1 + R_2 + R_3 \quad (4.6)$$

$$R = \frac{l_1}{k_1} + \frac{l_2}{k_2} + \frac{l_3}{k_3} \quad (4.7)$$

Where, l_1= Thickness of outer cover Aluminum sheet metal

l_2= Thickness of Insulation fiber wool

l_3= Thickness of inner cover Aluminum sheet metal

$k_{1=}$ Thermal conductivity of Aluminum sheet metal

$k_{2=}$ Thermal conductivity fiber wool

$k_{3=}$ Thermal conductivity of Aluminum sheet metal

l_1=l_3=1mm=0.001m

l_2=40 mm=0.040m

k_1=k_3= 205 W/mK

k_2=0.038 W/mK (Kulkarni & Rajput, 2013)

R=1.0526

U = $\frac{1}{R_{Total}}$ = 0.95 w/m^2oc

Substituting these values into equation 4.7 gives R=1.0526 m^2°C/W

The overall heat transfer coefficient is determined using equation 4.5 and is found to be U = 0.95 W/m^2°Ci

The convective heat transfer coefficient is calculated from the Nusselt number as follows (Ndukwu et al., 2013)

$$Nu = \frac{\text{hl}}{K}$$

$$k = is\ thermal\ condactivity\ of\ air$$

$$l = is\ the\ characteristic\ length$$

$$h = Heat\ transfer\ cofficent$$

$$Nu = \frac{hI}{K}$$

$$h = \frac{Nu \times k}{I} = \frac{118 \times 0.0025}{0.001} = 295 \frac{w}{m^2.℃}$$

Heat transfer through the wall consider all the wall are made of the same material thus, total surface area of wall is,

$$A_{total} = A_F + A_B + A_L + A_R + A_{Bo} + A_T \quad (4.8)$$

Where, A_F = Front surface area

A_L = Left side surface area

A_R = Right side surface area

A_B = Back side surface area

A_{Bo}= Bottom side surface area

A_T = Top side surface area

The surface area of the front, back, right, left, back and bottom sides is given in table 4.2 and substituting these values into equation 4.8 gives a total area of 3.6 m^2.

From the five years average meteorology data, the ambient temperature of Kombolcha for this project is taken as 28℃ and the average relative humidity is taken as 63%. The temperature required to preserve tomato inside the cold storage is recommended between 18℃ and 22℃.

Table 4. 3: Basic atmospheric condition data(Ayele, 2020)

Outside air DBT	+28℃
Cold Chamber DBT	18-22 ℃
Relative humidity	63%
Product Temperature	25℃ (At the loading Time)

The total heat transfer through the walls is determined from equation 4.3 as:

$Q_w = UA\ (CLTD)$ (Khakre et al., 2017)

$U\ = over\ all heat\ transfer\ cooficent(^{W}/_{m^2°C})$

$A = surface\ area(m^2)$

$CLTD = Cooling\ load\ \ Temprture\ diffrence$ (℃)

= 0.95 W/m^2℃ × 3.6 m^2 × (28 ℃- 18℃) = 34.2W.

Heat transmission through ceiling

The cold storage chamber ceiling is consisting of different layer of material so that overall heat transfer coefficient is calculated on the basis of given criteria and then heat transfer in equation (3.14) is calculated as(Bhatia, 2001).

$$Q\ =\ UA\ (To - Ti)\ W \qquad ()$$

Where

A =Surface area of the cabinet (m2)

U =Over all heat transfer coefficient (W/m^2 ^{o}C)

Ti =Inside temperature of cold storage air (^{o}C)

To =Outside temperature of atmosphere air (^{o}C)

Heat transfer through the ceil having the area of 0.56 m^2

$$U\ =\ 1/R\ =\ 0.95W/\ m^{2°}C$$
$$Q\ =\ 0.95x0.56x\ (28 - 15)$$
$$Q\ =\ 6.94W$$

4.2.2 Fruit and vegetable load

Commodity is warmer than the conditioned space. When it is loaded at the cold storage space, it will cool up to the required temperature. Specific heat multiplied by mass and temperature difference gives tomatoes cooling load (Ayele, 2018a).

$$Q_t = mC\Delta T \qquad (4.9)$$

Where, Q_t = Amount of heat energy needed to be extracted from tomato (J)

m = The mass of the product in kg

C = The specific heat of vegetables above freezing kJ/kg. K

ΔT = Temperature difference

The total mass of tomato is 100kg, the specific heat of tomato is 3.6kJ/kg. K, the initial temperature of the tomato is taken as 25℃ and the final temperature after colling is 20℃. By substituting these values into equation 4.9, the cooling load of tomato is 1800kJ.

4.2.3 Respiration load

Fruits and vegetables do not die at the moment of harvested because they have 65-95% of water. So, they have a live after harvesting and continue their living processes after harvested while in storage the more vital of these adjustments are produced by means, of respiration a process throughout which oxygen from the air combine with the carbohydrates in the plant tissue and results in the release of CO_2 and heat. The heat release called respiration heat. In such case heat gain is compute by the following equation (Jitendra Jayant, 2016)

$$Q = (M) \times (Respiration\ heat) \quad (4.10)$$

Where, Q_{res} = Quantity of heat in J

m = Mass the product in kg

The respiration heat of some products is given in table 4.5.

Table 4. 4: Heat of respiration of products(Gross et al., 2016).

Product	5ºC(mW/kg)	25ºC(mW/kg)
Apples	13–36	44–167
Strawberries	48–98	303–581
Broccoli	102–475	825–1011
Cabbage	22–87	121–437
Watermelon	*	51–74
Onions	10–20	50
Potatoes	11–35	13–92
Tomatoes	*	71-120
Carrots	20-18	0.05002
Lemon	7-10	0.01119

$$M = 100kg$$
$$Heat\ of\ respiration = 0.0955W/kg$$
$$Q = 100 \times 0.0955W/kg$$
$$Q = 9.55W$$

From table 4.5, the respiration heat of tomato is 95.5mW/kg = 0.0955W/kg. Substituting this value and m = 100kg into equation 4.10, the respiration load of Tomato becomes 9.55W.

4.2.4 Air change load

Air enters and exits the cold space during opening and closing of the cooler door for loading and unloading. This will cause the cold air inside the cooler to escape the cooler and warm air to enter the cooler. This creates additional load on the cooler known as air change load.

$Q_{ACL} = V \times ACH \times (h_a - h_f) \times \rho$ (Ayele, 2020) (4.11)

Where, Q_{ACL} = Air alternate load due to door opening infiltration and ventilation etc. (W)

V = Volume of cold room

ρ = Density of air

ACH = Air change per hour

Subscripts f and a denote cold room and ambient property, respectively.

The ACH value varies from 0.5 ACH for tight and well-sealed cold storage structures to about 2.0 for loose and poorly sealed constructions. For modern buildings the ACH value may be as low as 0.2 ACH(Tamrat et al., 2021). For this take the average of ACH 1.25. Corresponding to T_f = 20 ℃ and 92% RH value of h_f =41 kJ/kg same as T_a=25 ℃ and 63% RH value of h_a= 58 kJ/kg.

The volume of the cold room can be calculated as, V = L×W×H = 0.432m^3 and the density of air is ρ = 1.204kg/m^3 @20ºC. BY substituting these values into equation 4.11, the air change load of tomato becomes 11.05kJ.

$$V = 0.432m^3$$
$$\rho = 1.204\text{kg/m3}$$
$$ACD = 1.25$$
$$(ho - hi) = 26\ kJ/kg$$
$$ACL = (V) \times (ACH) \times (ho - hi) \times (\rho)$$
$$ACL = 0.432x1.25x(62 - 41)x970$$
$$ACL = 11.05kJ$$

4.2.5 Total cooling load

The total cooling load is the sum of the heat transfer through the walls, the heat load of tomato, respiration load and air change rate cooling load.

$Q_{total} = Q_w + Q_t + Q_{res} + Q_{ACL}$ (4.14)

=34.2W + 6.94w+9.55W+29w (1800kJ+ 11.05kJ)/Δt= 156.54W

Where, Δt is the time taken for a 100kg tomato to cool from 25ºC to 20ºC. Thus, the amount of power required to remove the required heat from the cooler will depend on the time taken to cool the product.

the flow velocity can be determined

$V = \frac{Re * \mu}{D.\ \rho}$ ……eqn (4.15)

Were,

V = flow velocity

Re = Reynolds number

μ = dynamic viscocity

D = diameter pipe

ρ = density of water

$$V = \frac{Re * \mu}{D.\rho}$$

$$= \frac{2200 * 0.001}{0{,}00939 * 998.23}$$

$$= 0.5\ m/s$$

And the volume flow rate can be determined by multiplying the area with the mass velocity(Soh et al., 2016).

$v \rightarrow flow\ rate = V * A$……. eqn (4.16)

Where,

V = Volume flow rate

A = area of Pipe

Equation 4.13 gives us a flow rate of 1.625 x $10^{-5}m^3/s$. The mass flow rate is a multiplication of the volume flow rate with the density.

$$m = V * \delta \quad \text{……eqn (4.17)}$$

Where,

m=mass flow rate

V = Volume flow rate

$$\rho = density\ of\ water$$

The mass flow rate from equation 4.14 is 0.016225 Kg/s. Now, we can calculate the heat transfer from the water to the cooler with the attained mass flow rate using equation 4.15.

$$Q = mcp\Delta T \quad \text{…….. eqn (4.18)}$$

Where m=mass flow rate

Cp = specific heat capacity of water

And ΔT is difference of the inlet and outlet temperature of water. The inlet temperature of water depends on the water temperature coming out of the evaporative cooler. And this is found between the wet bulb and dry bulb temperature of ambient air(Ndukwu et al., 2023). And the outlet temperature of water will be less than the initial temperature of tomato. For our initial calculation, we have taken the inlet temperature of water in to the cooler to be 17ºC. Therefore, the heat transfer will be;

$$= 0.016225 * 4184 * (23 - 17)$$
$$= 407.3\ W$$

Next, by equating this heat to the heat required to be removed from the cooler (the cooling load), we will get the time taken to cool the load (100kg of tomato) inside the cooler.

$$Q = 684\ W + \frac{1848.65Kg}{\Delta t}$$

Thus, by substituting Q with 407.3W, we get the time taken to cool 100kg tomato for a water inlet temperature of 17ºC to be 4546.357 Sec.

$$\Delta t = 1hr.16min\&57\ sec \approx 1hr\&17min$$

Figure 4.4 shows the variation of the cooling time with inlet temperature.

4.3 Selection of Cooling Pad

As section of the normal requirements, the efficiency of an active evaporative cooler depends on the water holding capacity and quantity of evaporation of water from the cooling pad. This is dependent upon the air velocity through the fan, pad thickness and the degree of saturation of the pad, which is a function of the water flow rate wetting the cooling pad. an effective cooling pad thickness depends on the amount of supply air from the fan and the amount of water flow rate. The effective thickness of pad reported are 20mm – 60mm (Taye S. Mogaji, 2011). In this work, kusha mat was selected for an efficient performance of the evaporative cooling system since it has good water holding capacity, high moisture content, and percentage dry basis, high bulk density reported (Zakari et al., 2016)

Factors to consider when choosing cooling pad materials:

- Availability: The evaporative cooling pad material should be locally available and should be cheap affordable for small-scale farmers.
- Moisture Content: The pad materials with high moisture content retention capacity should be selected.
- Water Holding Capacity: By definition, it is the ratio of the mass of water held at saturation to the initial mass of the material. The pad material should have good water holding capacity.
- the pad thickness is changed into and 100mm 75mm 50mm. $t = 100$ $v = L \times w \times t$

$$0.6 \times 1.2 \times 0.1m$$

$$= 0.072m^3$$

$$when \quad t = 75m$$

$$L \times w \times t$$

$$0.6 \times 1.2 \times 0.01$$

$$= 0.072$$

$$when \quad t = 50m$$

$$L \times w \times t$$

$$0.6 \times 1.2 \times 0.05m$$

$$= 0.036m^3$$

4.3.1. Mass balance on the cooling pad

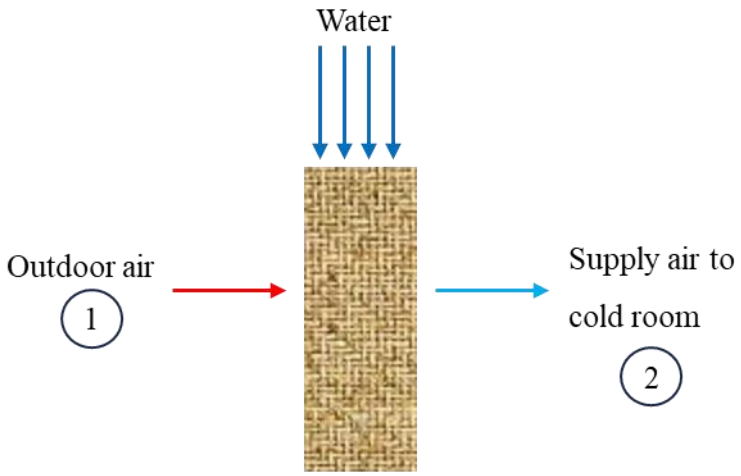

Figure 4. 2: Schematic of air and water flow through cooling pad

From figure 4.2, the dry air mass balance is

$$\dot{m}_{a1} = \dot{m}_{a2} = \dot{m}_a \tag{4.19}$$

The water mass balance is:

$$\dot{m}_{aw1} + \dot{m}_w = \dot{m}_{aw2} \tag{4.20}$$

From equation 4.14, $\dot{m}_{aw1} = \dot{m}_a \omega_1$ and $\dot{m}_{aw2} = \dot{m}_a \omega_2$.

$$\dot{m}_a \omega_1 + \dot{m}_w = \dot{m}_a \omega_2 \tag{4.21}$$

Where, $\dot{m}_{aw1}$ = the mass of water present in the air entering the evaporative cooler

$\dot{m}_{aw2}$ = the mass of water present in the air leaving the evaporative cooler

$\dot{m}_w$ = the mass of water added to the air

$\dot{m}_a$ = mass flow rate of air entering the evaporative cooler

ω_1 and ω_2 = the specific humidity of air entering and leaving the cooler, respectively.

4.4 Fan selection

Fans are powered machines used to create a flow of air. A fan consists of a rotating arrangement of vanes or blades, which act on the air. The rotating assembly of blades and hub is known as an impeller, rotor, or runner and usually it is contained within some form of housing, or case. This may direct the airflow, or increase safety by preventing objects from contacting the fan blades.

To determine the capacity of fans in evaporative cooling system, the volume of air that needs to be circulated inside the cold storage should be determined first. The amount of air needed to produce the required cooling can be determined from the cooling capacity.

$$Q = \dot{m}_a C_P \Delta T \quad (4.22)$$

Where, Q = the total cooling capacity

$\dot{m}_a$ = mass flow rate of cooling air

C_P = specific heat capacity of the air$s$ room temperature which is 25^0C. Thus, substituting Q = 156.54W, ΔT = 7℃ and C_P = 1.012kJ/kg. K into equation 4.13, the mass flow rate of the cooling air becomes $\dot{m}_a$ = 0.018kg/s.

The volume of air can be determined as:

$$\dot{V} = \frac{\dot{m}_a}{\rho} \quad (4.23)$$

Substituting $\dot{m}_a$ = 0.018kg/s and ρ = 1.168kg/m^3, the volume flow rate of the air needed for cooling becomes $\dot{V}$= 0.924 m^3/min.

The capacity of fans is specified in terms of cubic feet per minute (cfm) and 1cfm = 0.028 m^3/min. 0.924 m^3/min becomes 33cfm and a fan with the nearest cfm is selected and its specification is shown in table 4.6.

Figure 4.3: Fan

Table 4.5: Specification of the selected fan (Source: Orion Fans Catalogue)

Model Number	0089733-12HB	0089733-24HB
Part Number	104141001	104241001
Nominal Voltage	12 VDC	24 VDC
Voltage Range	10.s - 13.2 voe	21.6 - 26.4 voe
Nominal Current	0.78 A	0.35 A
Input Power	9.36 W	8.40 W
Rated Speed (RPM)	4000	4000
Airflow (CFM)	33	33
Noise Level (dB)	56	56

4.5 Pump selection

A pump is used to circulate the water from the storage tank with small pipes and spraying the water over the cooling pad. In order to determine the right size of the pump for the evaporative cooler, the required rate of water supply and the pressure drop should be determined. The rate of water supply to the cooling pad is determined in section 4.3.1 with equations From equation 4.15, ω_1 and ω_2 are the specific humidity of air entering and leaving the cooler, respectively. From psychrometric chart, since the air enters at 28℃ DBT and 62% RH ω_1 = 0.01425 kg/kg H_2O and assuming the air leaves the cooler at 95% RH, ω_2 = 0.0165 kg/kg H_2O. Substituting these values and the mass flow rate value obtained from equation 4.16 which is, $\dot{m}_a$ = 0.548kg/s into equation 4.15, the mass of water supply to the evaporative cooler $\dot{m}_w$ =

0.0405kg/min. Thus, the minimum volume of water that should be supplied to the evaporator cooling pad becomes, $\dot{V}_{\omega}$= 4.05 × 10^{-5} m^3/min.

The pressure drops inside the water circulating tube (ΔP_t) and due to the 90º bend (ΔP_b) can be determined using equations 4.18 and 4.19 respectively.

$$\Delta P_t = f \frac{L}{D} \frac{\rho v^2}{2} \quad (4.24)$$

$$\Delta P_b = K_f \frac{\rho v^2}{2} \quad (4.25)$$

Where, L is the length of the tube

D is the diameter of the tube

ρ is density of water

v is velocity of the water

f is the friction factor which depends on the flow type (laminar or turbulent)

K_f is the pressure factor loss

To determine whether the flow is laminar or turbulent, the Reynolds number should be determined:

$$Re = \frac{vD\rho}{\mu} \quad (4.26)$$

The velocity of water is determined from $\dot{V}_{\omega} = v\,A = v\frac{\pi}{4}D^2$. Taking the diameter of the tube as 24mm, the velocity of the water is 0.0896m/s. And from water property table, we find that the dynamic viscosity and density of water at room temperature and at elevation of 1842m (elevation of Kombolcha) to be, μ,= 0.001 $kg/m.s$ and density= 998kg/m^3. Thus, the Reynolds number Re = 2164 which is laminar flow. For laminar flow the friction factor $f = 64/Re$ = 0.0296 and K_f = 0.9. Substituting these values into equation 4.18 gives $\Delta P_b = 3.46Pa$ and $\Delta P_b = 3.61Pa$. The total pressure drop is $\Delta P_b + \Delta P_b = 7.07Pa$.

The pump required for solar evaporative cooling system should be able to deliver the maximum flow rate and overcome the calculated pressure drop. These specifications show that the pump to be used for the evaporative cooler under design is a submersible DC pump with a rated voltage of 12V. This type of pumps can pump water at low flow rate and low pressure. There are different

types of submersible DC pumps in the market today. One example of such a pump can be seen in figure 4.4 and its specifications are shown in in table 4.7.

Figure 4. 4: Mini DC water pump

Table 4. 6: Pump specification

Model	Product Code	Max Flow Rate (UMin)	Max Water Head (m)	Voltage (VDC)	Current (A)	Starting Voltage (VDC)	Power (W)
TSSIPV	TSS.A12 5PV	8.4	1.6	12	0.41	2	5
	TSS.A 12-10PV	10	2.4	12	0.33	2	10
	TS5-A 12·15PV	12.6	3.2	12	1.25	2	15

4.5.1. Storage tank and water distribution network sizing

The water is stored in a tank and is circulated and distributed on the cooling pad with a water distribution pipe with help of the pump. In the previous section we found that the amount of water evaporated into the air $\dot{m}_w$ = 0.0405kg/min. Based on this, the amount of water evaporated per hour will be 2.43kg and the amount becomes 58.32kg/day. From this, the volume of the required water per day becomes 0.059m^3 which is 59 liters. The volume of the storage tank should be large enough to store 59 liters of water. The water is distributed with water distribution pipe and the pipe should be light in weight, corrosion resistant, and low in cost. PVC pipe perforated at an interval of 5cm can be used to spray the water evenly over the cooling pad.

4.6 Solar panel and battery selection

Total power consumption of the Evaporative cooling system can now be determined by adding the power consumption of the pump and the fan, 5W + 9.36W = 14.36W.

For selecting our solar panel, in addition to the total power required, we also need to determine the solar radiation of Kombolcha year-round. This can be estimated from previous solar data taken in Kombolcha. This data will also assist us in determining the possible operation hours of the evaporative cooler under direct sun for each month of the year and help us determine the appropriate battery for the system.

Tilt angle shows the orientation of the solar panel for optimum performance (power output) from the received solar radiation. It is the angle between the panels and the horizontal plane. This angle is south oriented in the northern hemisphere and north oriented in the southern hemisphere. Tilt angle varies between 0^o and 180^o. For best average summer performance, a collector should be mounted at approximately $\varphi - 15°$, and for best average winter performance, it should be mounted at $\varphi + 15°$.

The conversion of the solar energy into useful power is done by battery and invertor. The solar radiation is converted into electrical energy by the solar panels. This energy is stored in the batteries and can be directly used for DC loads. But if the loads are AC, it should be converted into AC with an inverter. In this research, the selected fan and pump are DC type and the stored energy in the battery can be directly supplied to these electrical devices.

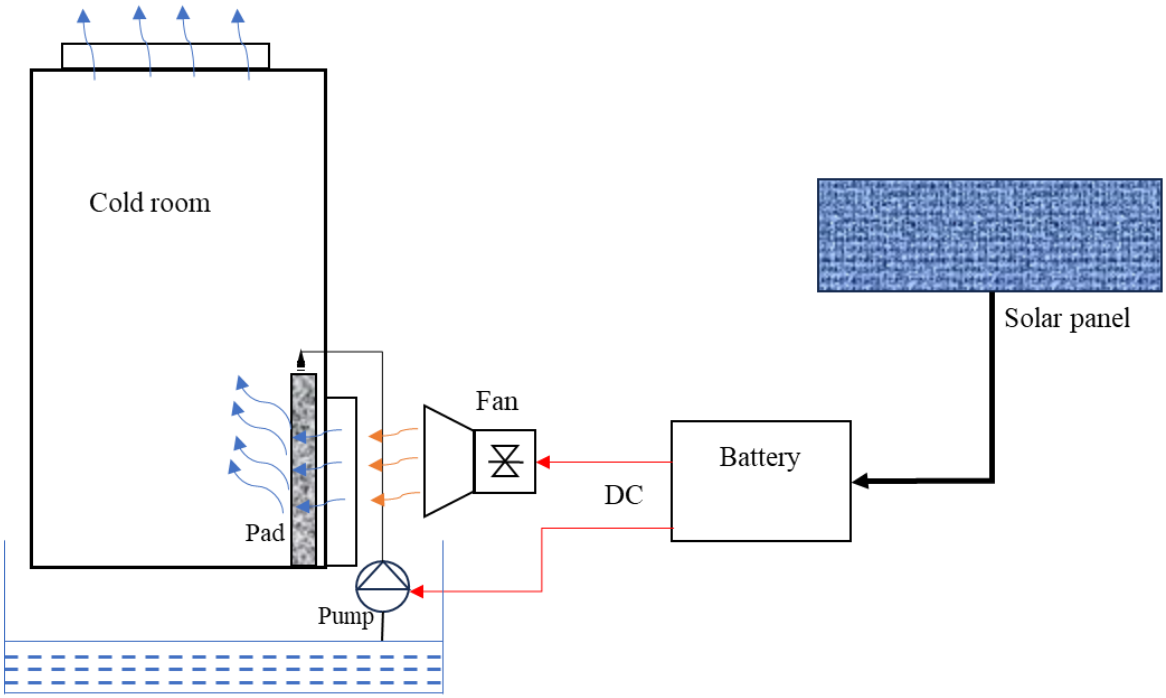

Figure 4. 5: Schematic of solar panel, pump and fan arrangement.

4.6.1. Battery selection

Table 4. 3: Battery sizing table

No.	Equipment	Mode	Voltage	Current Draw	Time Active/Hour	Avg Current
1	Pump	Running	12V	0.41A	1	0.41A
2	Fan	Running	12V	0.78A	1	0.78A
					Total Average Current	1.19A
	Desired Run Time in Days				17	17 Total Hours
	Total Average Current * Total Hours = Calculated Battery Size					20.23 Amp Hours
	Efficiency Factor			1.25	* Calc Battery Size	25.29 Amp Hours
					Next Available Battery Size	30 Amp Hours

The battery operating hour (discharging mode) is taken to be 17 hours a day. This is based on the minimum monthly average solar radiation of Kombolcha.

4.6.2. Solar panel selection

The selected solar panel should be enough to run the pump and the fan while charging the 30AH battery. Thus, first we need to calculate the current required to charge the battery. From the solar radiation data of Kombolcha, we have an average of 7hrs good solar radiation (more than 333W/m^2) in a day. This indicates that our battery should be fully charged with in 7hrs in order to have a continuous operating evaporative cooler on battery for the remaining 17hrs.

The current required to charge a 30AH battery is calculated using equation 4.21.

$$I = AH / H \quad (4.27)$$

Where, I is the current required, AH is the battery ampere hour and H is the hour taken for fully charging the battery. Thus, it will require 4.3Amps of current to charge the 30AH battery in 7hrs. But batteries are not 100% efficient. For example, lead-acid batteries have around 60% efficiency. Therefore, considering 40% battery loss, the current required to fully charge the 30AH battery in 7hrs will be, 4.3Amps *1.4, which is 6Amps. After this, we can select the solar panel required to run the designed evaporative cooler using table 4.9. In the table we have considered using both the 30AH and 150AH batteries. The 150AH battery is selected based on the requirement analysis to run the cooling system for one week with one full charge. This will be necessary if the tomato cultivation period is during the winter season. But most of the cultivation period in kombolcha is around the summer season. Thus, the 30AH battery is the best match for our solar evaporative cooling system.

Table 4. 7: Selection of solar panel

Battery Size in Amp Hours	30 Amp Hours	150 Amp Hours
Total Recharge Time in Hours	7 Hours	7 Hours
Calculated Charge Current: (Battery Amp Hours/Charge Time) *1.4	6 Amps	30 Amps
Average system Current	1.19 Amps	1.19 Amps
Total Current Required: Charge Current + Average System Current	7.19	31.19
Required solar panel output: Total Current Required * 12.0 Volts	86.28 Watts	374.28 Watts

Thus, the next solar panel size for the 86.28W requirement would be a 100W solar panel. But a 100W solar panel doesn't always give a 100W electrical power output. The number is an estimated range of the expected output when all conditions are perfect. These conditions are known as STC (Standard Test Conditions) and are determined in a laboratory. Standard test conditions for PV modules are 25°C and 1000W/m². If these perfect conditions are achieved, a panel of 100W rating will generate exactly 100W of electricity. These are laboratory tests. But performance of the modules in the real world depends on the solar panel's efficiency, its orientation and its location.

There is no definitive way to find the exact electrical power output of a solar panel, but a good estimation can be achieved by using the global formula shown in equation 4.22.

$$\text{Solar Panel Output} = \text{Wattage} \times \text{Peak Sun Hours} \times 0.75 \quad (4.28)$$

The solar panel output is determined in KWh/day. As, discussed earlier, the wattage of the solar panel is the maximum output of the solar panel at STC. And all the energy efficiency of solar panels (15% to 25%), type of solar panels (monocrystalline, polycrystalline), tilt angles, and so on are already factored into the wattage. The 0.75 factor in equation 4.22 refers to the 25% electrical loss. These losses occur when the electricity generated by the solar panels is passed through batteries, inverter, DC and AC cables. The peak sunshine hour is the number of hours in a day for a particular location when the average solar insolation reaches STC. Because, the solar rated output can reach up to 150% in the afternoon and only around 20% in the evening and morning time. This number will vary through the months.

To get a more precise result, the average solar insolation to STC ratio can be used instead of solar peak hour. For example, the average solar insolation for Mar 15, 2021 according to NMA, is 446W/m², considering only 7hrs of sunshine, from 3:00AM to 4:00PM. Thus, the average solar insolation to STC ratio for the 7hrs become 44.6%. Substituting this in equation 4.19, we get;

$$\text{Solar Panel Output} = \text{Wattage} \times 44.6\% \times 7\text{hrs} \times 0.75$$

The required solar panel output for the 7 sunshine hours is already determined from table 4.9. The result shows that, 86.28W x 7hrs, i.e 0.6KWh/day is required for the system to work 24hrs a day. The estimated solar insolation is taken by averaging the last five years solar data for Kombolcha. Figure 4.5 shows the final electrical output in KWh/day for a 100, 200, 250 and 300 wattage panels based on the equation discussed above.

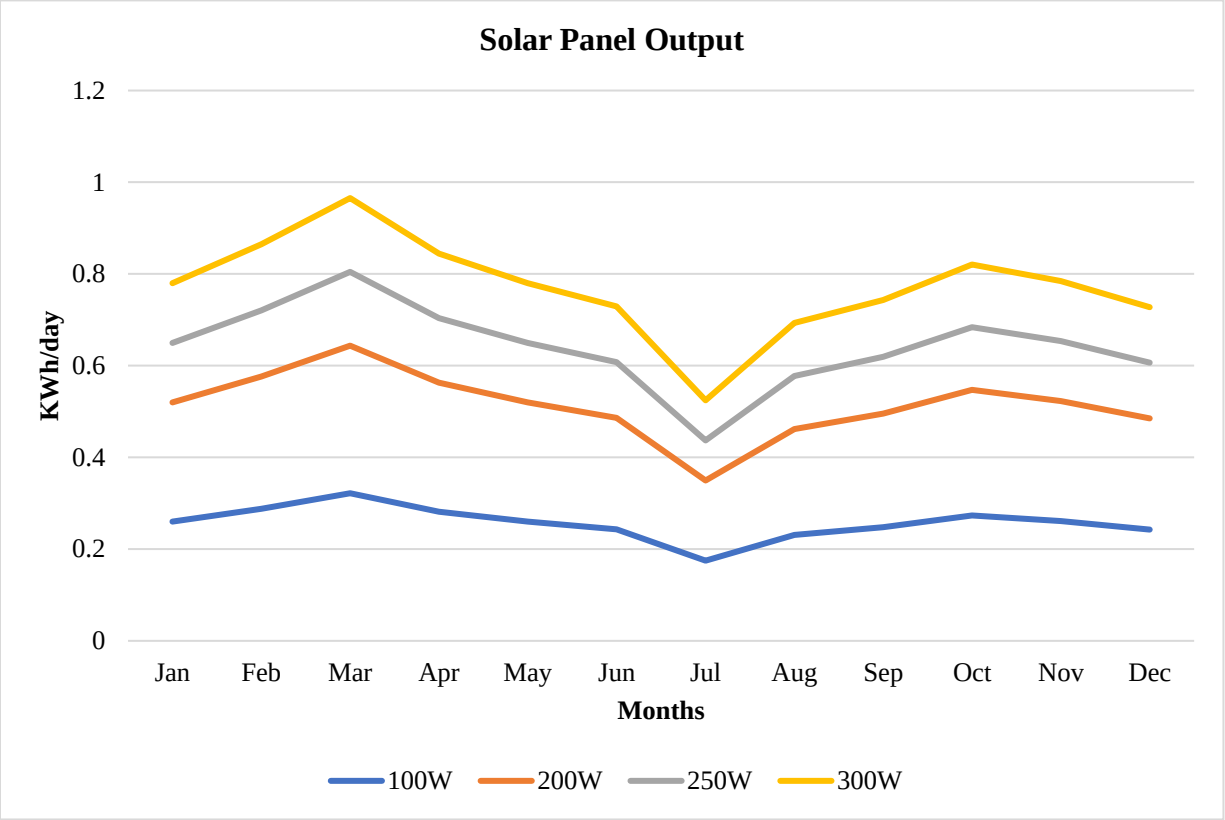

Figure 4. 6: Solar panel output for different watt panels

Thus, from figure 4.6, we find that the 250Watt solar panel is the more suited choice for our system. The graph shows that, for two months, the output of the 250W solar panel, drops below the required energy for the system. But these months are July and August, which are rainy months of the region, and we do not require refrigeration system for these months because they are farming and seeding months for Kombolcha.

The commercial size of the 250W solar panel is 1.65m by 0.99m. The 30AH battery will be fully charged with in the 7hrs of sunshine using the 250W solar panel and make sure that the cooling system works 24hr a day by powering the system after sunset. There is much more involved in battery selection considering the power source and charging system that is not covered in the selection criteria. The type of battery should be suited for several charge/discharge cycles, the battery installation should prevent it from overheating and more importantly there should be a regulator system between the charging system and the battery that prevents overcharging and other battery killing operations.

4.7. Performance parameters of the Evaporative cooler

The performance of a direct evaporative cooling system is evaluated in terms of its cooling capacity, effectiveness and evaporation rate of water (Laknizi et al., 2019).

The evaporative coolers cooling capacity in the pad is evaluated in terms of the temperature drop of the air.

$$Q_{c_{Pad}} = \dot{m}_a C_P [T_1 - T_2] \quad (4.29)$$

Where $\dot{m}_a$ is the flow rate of the air (kg/s), C_P is the specific heat capacity of the air, T_1 is the inlet dry bulb temperature and T_2 is the outlet dry bulb temperature.

The mass flow rate of the air can be determined by multiplying the air velocity by density of air and cross-sectional area of the material.

$$\dot{m}_a = \rho v A \quad (4.30)$$

The cooling effectiveness is the ratio of the inlet and outlet air temperature difference and the inlet dry bulb and wet bulb temperature difference.

$$\varepsilon = \frac{T_1 - T_2}{T_1 - T_{\omega_b}} \quad (4.31)$$

The coefficient of performance of the cooler is determined by calculating the ratio of the heat removed from the cooler to the work done to remove the heat. The input energy is the energy supplied by the solar panel to the fan and pump.

$$COP = \frac{Q_{cpad}}{P_{fan} + P_{pump_P}} \quad (4.32)$$

CHAPTER FIVE

5. SIMULATION

5.1. Simulation procedure on ANSYS

Ansys Fluent is used to create advanced physics models and analyze a variety of fluids phenomena in a customizable and intuitive space. Thus, the heat transfer inside the cold storage of the solar evaporative cooler due to the evaporation of water from the cooling pad is simulated using ANSYS 2023 R1 software. The simulation is done considering the cooling chamber is empty (No-load). The steps taken for the analysis of the heat transfer inside the cold storage is as follows.

The simulation procedure is described as follows:

1. Geometry creation: the geometry of the evaporative cooler is created using the dimensions from the design. To study the effect of the thickness of the pad on the performance of the evaporative cooler, three pad thickness are considered; 50mm, 75mm and 100mm.
2. Meshing: meshing of the evaporative cooler is done on ANSYS meshing.
3. Setup: the boundary conditions, initial conditions, materials, the model used are specified in this step. After specifying these conditions, the solution is initialized and the calculation is started.
4. Results: after the calculation is completed, the results of the simulation are collected.

CFD methods consist of numerical solutions of mass, momentum, and energy conservation. The governing equations for the simulation are manipulations of the conservation laws of fluid mechanics.

Continuity equation: $\nabla . \rho \vec{V} + \frac{\partial \rho}{\partial t} = 0$ (5.1)

Momentum equation: $\frac{\partial \vec{v}}{\partial t} + (\vec{v} . \nabla)\vec{v} = \frac{1}{\rho}(-\nabla P + \mu \nabla^2 \vec{v})$ (5.2)

Energy equation: $\left(\rho C_p u \frac{\partial T}{\partial x} + \rho C_p v \frac{\partial T}{\partial y} + \rho C_p w \frac{\partial T}{\partial z}\right) = K \nabla^2 T$ (5.3)

The simulation is done by considering three pad thicknesses (50mm, 75mm and 100mm), at four different dry bulb temperature (25℃, 27℃, 29℃, and 33℃) of air at the inlet (environmental

conditions), and inlet velocities of 0.5m/s, 1m/s, 1.5m/s ,2m/s and 2.5m/s. The overall simulation procedure is shown in table 5.1 as follows.

Table 5. 1: Simulation procedure

DBT of air (℃)	Velocity of air (m/s)
25	0.5
	1
	1.5
	2
	2.5
27	0.5
	1
	1.5
	2
	2.5
29	0.5
	1
	1.5
	2
	2.5
33	0.5
	1
	1.5
	2
	2.5

Each simulation is done for dry bulb temperature of 25℃, 27℃, 29℃ and 33℃ i.e,

- At the inlet DBT of 25℃ and velocity of 0.5m/s are specified for a pad thickness of 50mm and the temperature drop of the air at the outlet is recorded. This simulation is repeated by changing the velocity of air to 1m/s, 1.5m/s, 2m/s and 2.5m/s and the outlet temperature is recorded for each inlet velocity.
- Then the DBT at the inlet is changed into 27℃, 29℃, 33℃ and the above step is repeated for each temperature.
- Next the pad thickness is changed into 75mm and 100mm in the geometry and the above two steps are repeated for each pad thickness.

5.1.1 Starting ANSYS

The simulation is done on ANSYS 2023 R1 using ANSYS Fluent. Thus, after choosing and opening the ANSYS Workshop, we drag the 'Fluid flow (Fluent)' system analysis from the toolbox and place it on the project schematic display area.

5.1.2 Creating geometry

The geometry is created using Design Modeler. Double clicking on the 'Geometry' in the project schematic will open the Design Modeler. The cold storage is a rectangular box which is created in ANSYS geometry using the extrude command. Next, the 'Thin' command is used to create the cold storage with a void space inside from the rectangular box geometry. After this, the openings for the inlet and outlet of air on the cold storage are created using the 'Extrude Cut' command and the cooling pad is created near the inlet inside the cold storage as shown in Figure 5.1. The dimensions from the design in chapter four are used when creating the geometry.

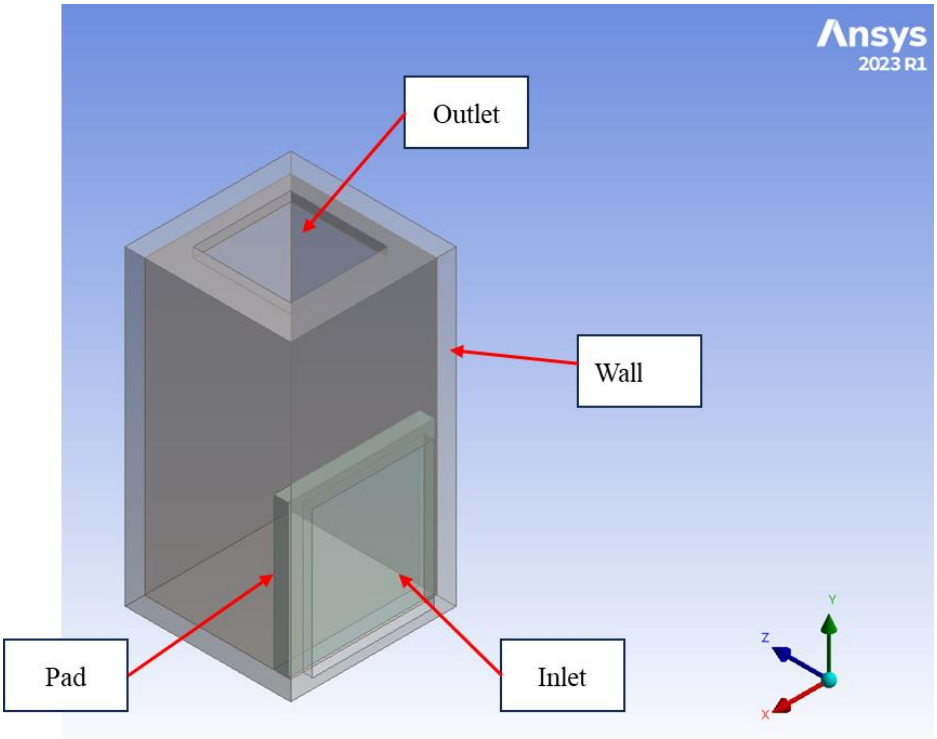

Figure 5. 1: ANSYS cold storage geometry

ANSYS considers the void space inside the cold storage as vacuum. Thus, the space inside the storage has to be filled with and assigned letter on in the setup stage as 'Air'. We will use the fill command for this. Figure 5.2 shows the geometry with the filled air inside the cold storage.

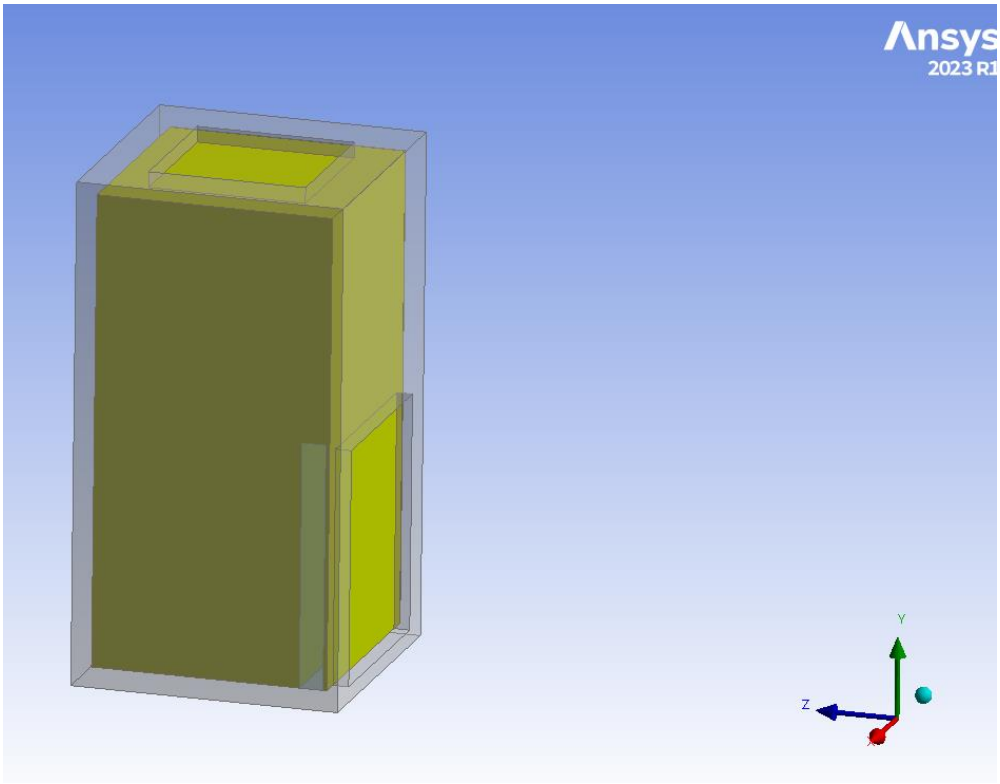

Figure 5. 2: Cold storage geometry with air inside

Finally, before quitting our geometry interface, we name our parts and assign solid to the cold storage body and fluid to the air inside. Then, by selecting the two bodies and right clicking on them, we chose 'form new part' on the tree outline. This will consider the two bodies as one part during meshing and will make us a conformal mesh. The tree outline displays one part and two bodies as shown the figure below.

5.1.3 Mesh development

We close the Design Modeler and open the meshing interface by double clicking on 'Mesh' on the project schematic. Here, we will click on the 'Generate Mesh' command. This will create the default mesh developed by ANSYS. The mesh is a conformal mesh since we have told ANSYS to consider the two bodies as one part during meshing, as shown in figure 5.3.

Conformal mesh means that each node at the two bodies is connected at the point of intersection between the two bodies. And ANSYS defines this as, every node on one side of the interface can be matched with a node on the other side of the interface with a very low tolerance. A conformal

mesh is required to simulate conjugate heat transfer, so that we can calculate the convection as well as the conduction heat transfer effects more accurately.

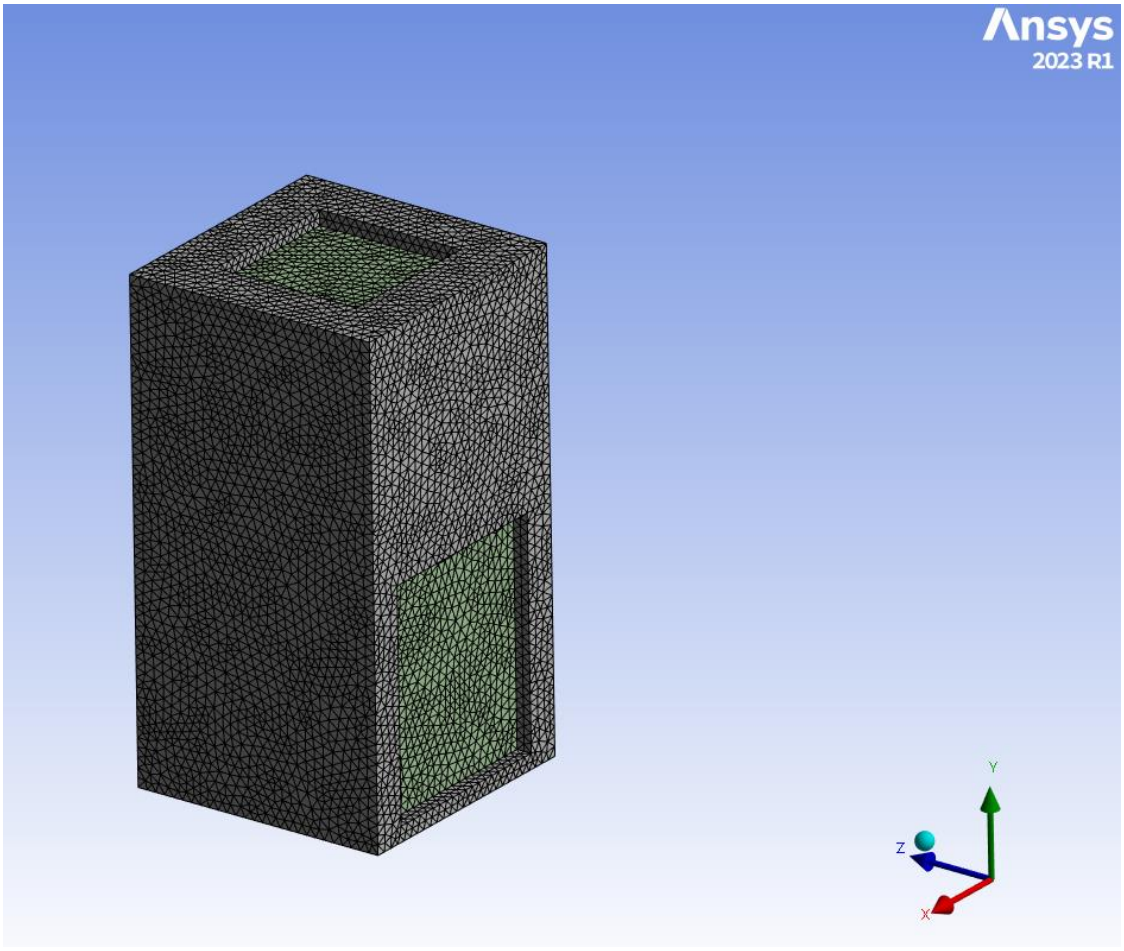

Figure 5. 3: Conformal mesh

The mesh developed is a combination of wedges and hexahedra elements. The mesh has a total of 34722 nodes and 176825 elements, with a maximum element size of 0.025m and a skewness of 0.9.

Next, we name the different surfaces of the bodies and the bodies itself that are used for the physics setup in the next step. This is done on the mesh interface by selecting the surfaces or bodies we want to name and by clicking ‘N’ on our keyboard. This will open the naming box and we can assign any name to the selected parts. Thus, the top opening of the cold storage is named ‘Outlet’, the opening at the right bottom is named ‘Inlet’ and the cooling pad is named as pad. The outer

surface of the cold storage is named 'Wall' and the two bodies (domains) are named Cold room and Air.

5.1.4. Grid independency test

To ensure that the solution is accurate regardless of the mesh size, a mesh independency test is done by varying the element size. The temperature of the air at the outlet is checked for each mesh size as shown in table 5.2. Four different element sizes are considered and the outlet temperature for each simulation shows that, the temperature recorded at element sizes of 0.025m and 0.015m are close. Therefore, element size of 0.025m is selected for the simulation to save computational time that the element size of 0.015m. The simulation is done at 25℃ inlet dry bulb temperature, 100mm cooling pad thickness and inlet velocity of 0.5m/s.

Table 5. 2: Grid independency test.

Element size (m)	Number of nodes	Number of elements	Temperature (℃)
0.045	8429	41711	19.86
0.035	15822	79008	19.57
0.025	34722	176825	19.23
0.015	176825	728316	19.23

After finish naming the meshing interval is closed and we proceed to the setup by double clicking on the 'Setup' in the project schematic.

5.1.5. Setup and Solution

In the setup interface we chose the physics used for analyzing the simulation and assign all the boundary conditions required. On the general setup we make sure that the analysis is a steady state analysis and select the gravity. This will open an input box for the magnitude and direction of the gravity we require in our analysis. Thus, we write ($-9.81 m/s^2$) value on the Y direction since our geometry is positioned on the ZX plane. On the Model toolbar, we select 'Energy' and make sure that it is on. This is required for ANSYS to analyze the heat transfer and temperature distribution. The multiphase flow model is also turned on and evaporation-condensation phase interaction is used since the water from the pad is evaporated when the air passes through it. The flow is selected laminar by default so we close the Model toolbar and proceed to materials. Here, from the fluent

database, Aluminum is assigned to the cold storage body, air to fluid flowing inside and the pad is modeled as a porous media containing water.

The boundary conditions in the inlet are specified based on table 5.1. Air entering velocity and temperature is inserted in the inlet setup and output pressure is inserted in the outlet setup. The convective heat transfer on the body is inserted for the wall surface setup. This is inserted in the form of W/m^2 of wall surface area.

Now, we proceed to the solving method and chose the 'Coupled' method. The coupled scheme obtains a robust and efficient single-phase implementation for steady-state flows, with superior performance compared to the segregated solution schemes. Then, the solution is initialized using a standard initialization method. The initial conditions inside the cold storage and the initial condition of the pad are specified.

Finally, we start the analysis of the solution by double clicking on the 'Run Calculation' tab and selecting the number of iterations we require for the calculation and pressing the 'Calculate' command. This will automatically start the iteration process and the residual graph will be displayed. Residual graph is the difference between the previous result and the new calculated value based on the previous result. The aim is to maintain this difference as minimum as possible. By default, ANSYS assigns this` difference to be 10^{-3}. Thus, the iteration will stop when these values reach 10^{-3} or when the number of iterations given by the user is reached. The figure below shows the residual graph of our calculation at the end of the iteration.

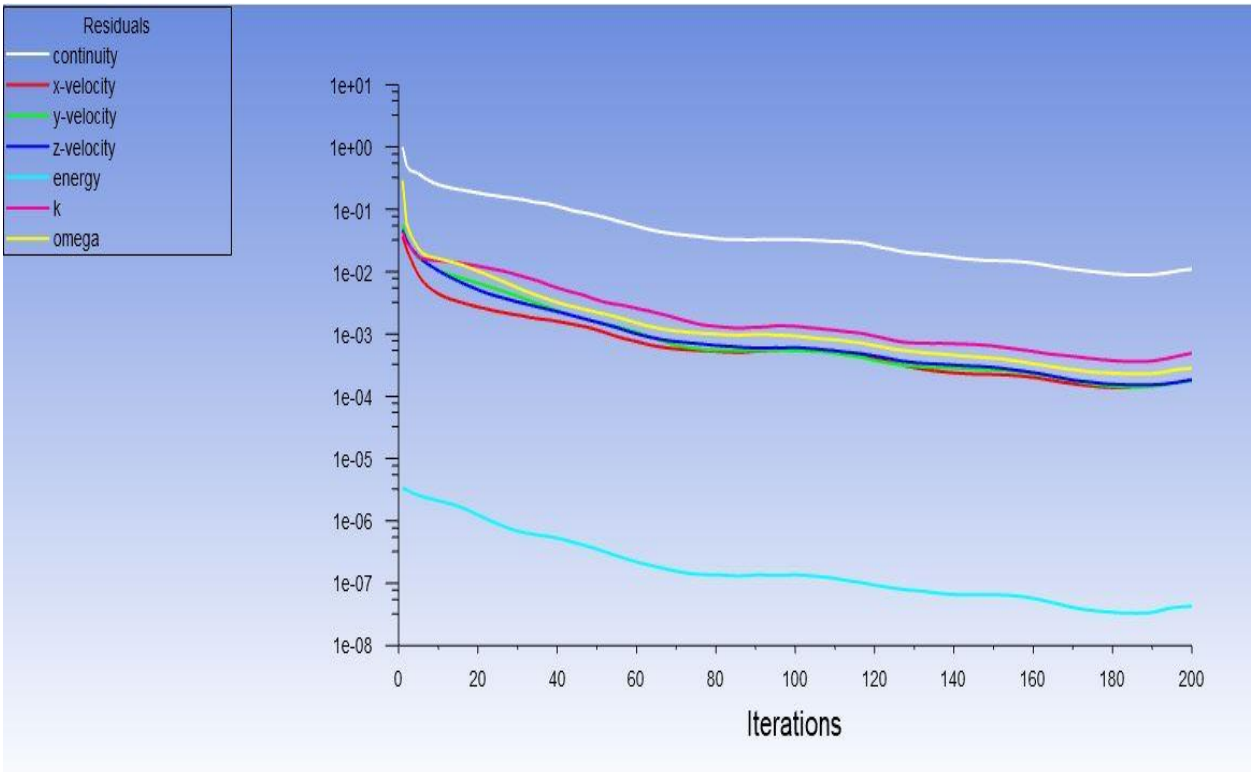

Figure 5. 4: Residual graph

5.1.6. Results

On the project schematic we will double click on the 'Result' tab and the fluid flow (Fluent) CFD post process interface opens. This interface helps us simulate the pressure, temperature, velocity and flow of the air inside the cold storage. This can be done in the form of contours, vector and streamlines and weighted averages.

In order to clearly show the above parameters on the flowing fluid, we need to create plane surfaces that intersect the cold storage at the required location. Increasing the contour lines gives us the detailed difference in parameters on the flowing fluid.

CHAPTER SIX

6. RESULT AND DISCUSSION

The results of the simulation and discussion of these results are presented in this section. The pressure, velocity and temperature contours showing the distribution of these variables and the performance of the evaporative cooler are presented and discussed.

6.1. Pressure, velocity and temperature contours

The contours showing the distribution of pressure, temperature and velocity inside the cold storage are presented in this section. The contours are plotted from the simulation when the inlet velocity is 0.5m/s, inlet temperature is 25℃ and pad thickness of 100mm.

6.1.1. Pressure contours

The first analysis we see on the result section is the pressure of the fluid inside the cold storage. The ANSYS software output of the final pressure of air inside the cold storage can be displayed in many forms. To get a detail understanding of how the air pressure behaves inside the storage, we have used contours as shown in figure 6.1. But the more descriptive was the display of the result on a plane created at the center of the storage, figure 6.2. As figure 6.1 and figure 6.2 shows, the pressure of the air inside the cold storage becomes greater at the corners of the storage and the pressure becomes lower around the outlet of the cold storage. The high pressure at the corners of the storage is due to the effect of resistance from the wall and the lower pressure at the outlet is due to the pressure becoming at equilibrium with the outside air.

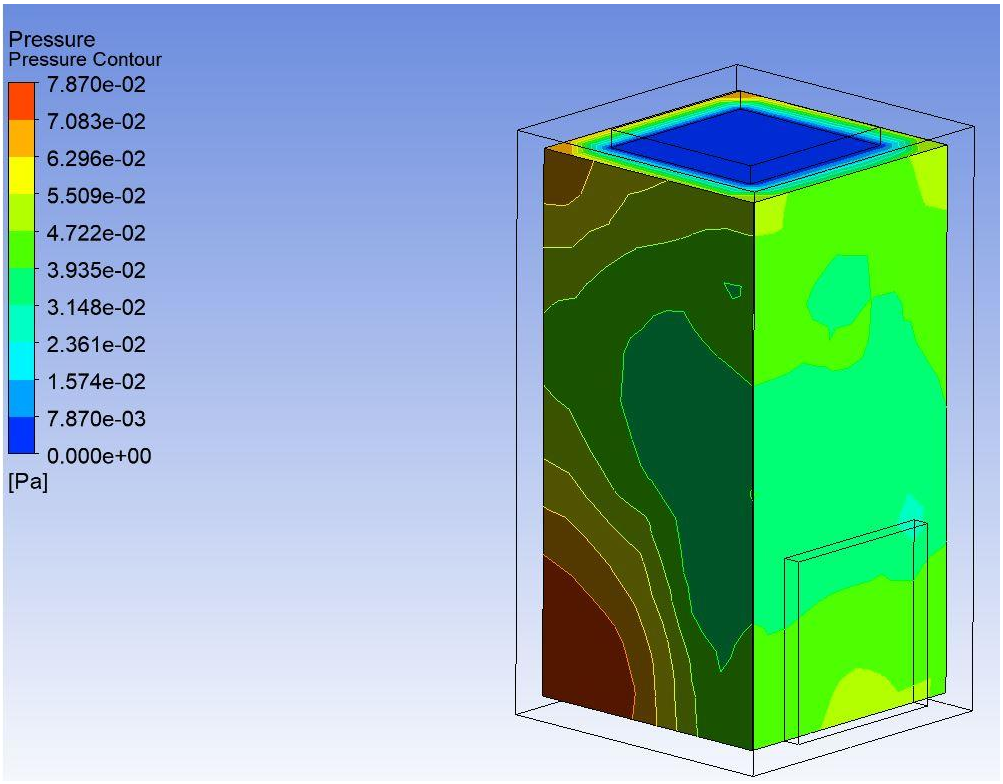

Figure 6. 1: Pressure contour inside the cold storage

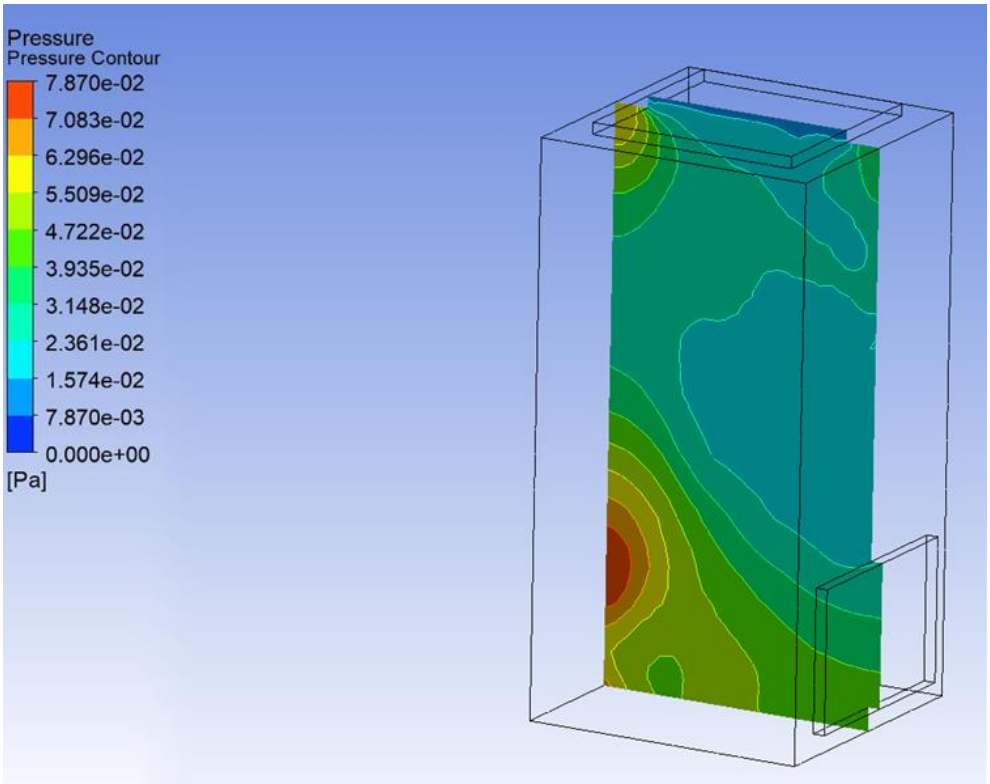

Figure 6. 2: Pressure displayed on a plane inside the cold storage.

6.1.2. Velocity contour

The next parameter we see here is the velocity of air inside the cold storage. Figure 6.3 shows the velocity contour on a plane inside the cold storage. Since, the inlet and outlet openings of the cold storage are equal in size, the velocity of air entering the storage and leaving the storage are nearly the same. Here on the simulation also the general theory applies. But the velocity inside the cold storage will differ with location. The flow behavior of air inside the storage is also studied in ANSYS using velocity streamlines as shown in figure 6.4. the velocity streamlines show how the air is distributed inside the cold storage when it flows from the inlet to the outlet.

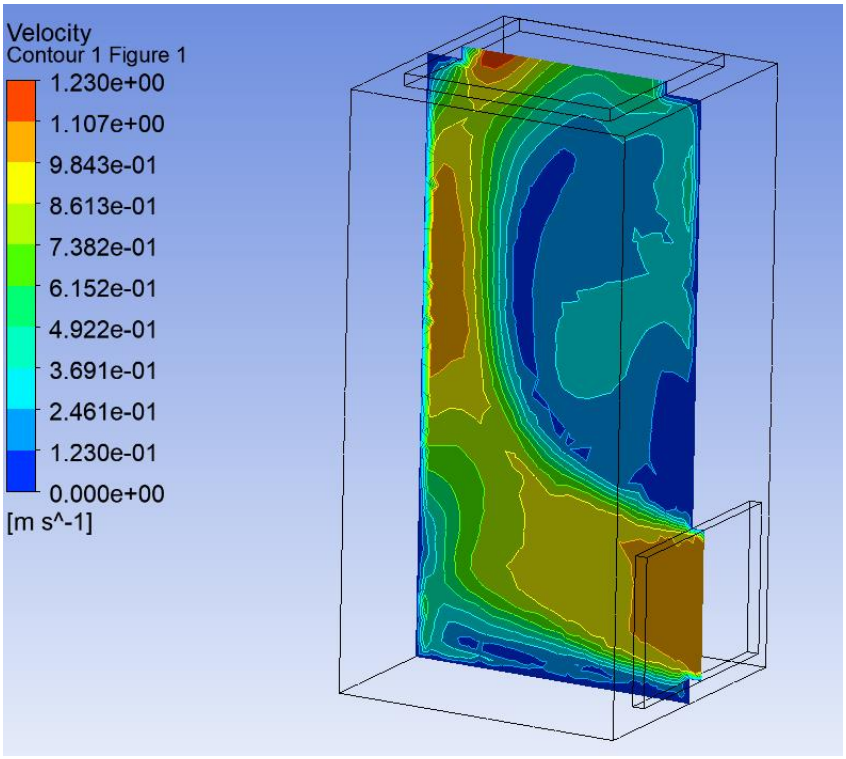

Figure 6. 3: Velocity contour

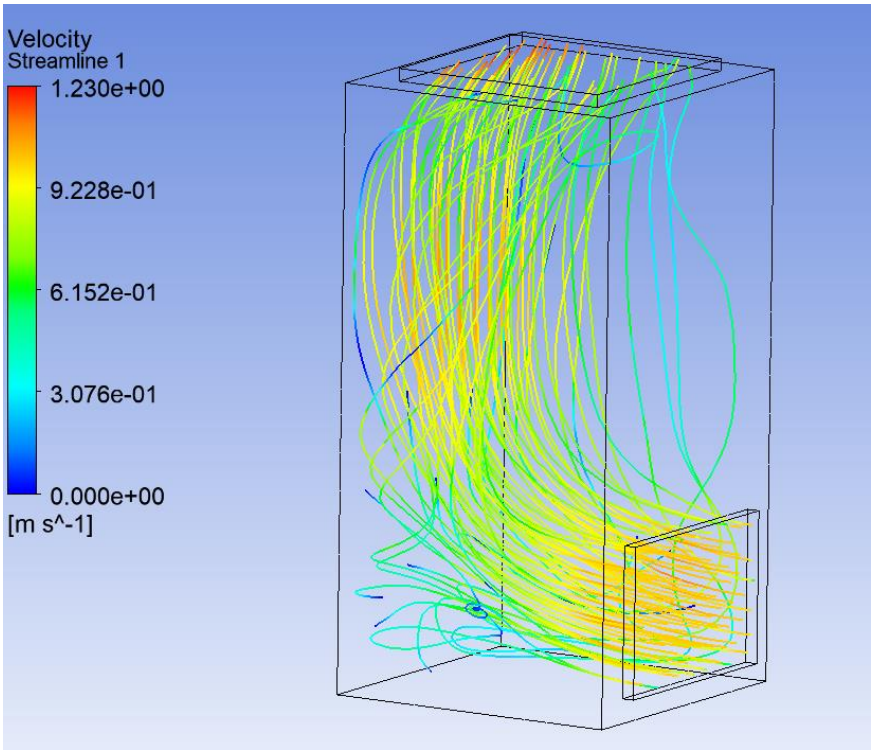

Figure 6. 4: Velocity streamline.

6.1.3 Temperature contour

The third analysis we made using ANSYS on our Evaporative cooler is temperature distribution inside the cold storage. This analysis is very important as it simulates which area inside the cooler gets cooled first and help us identify the amount of heat absorbed by air as it passes through the cooler. The temperature distribution inside the cold storage is shown in figure 6.5 and figure 6.6 shows the temperature distribution on a plane. From the figures, the temperature of the air inside the cold storage is around 292K (19℃) which is seen as blue color. In figure 6.5, the lightly yellowish green color observed on the outer surface of the cold storage is due to the effect of external convection.

Using equation 4.15, we can calculate the heat transfer from the cooler to the water using its inlet and outlet temperature. Thus, the equation will give us a result of 435.7W which is close to the value obtained in the design part, 407.3W.

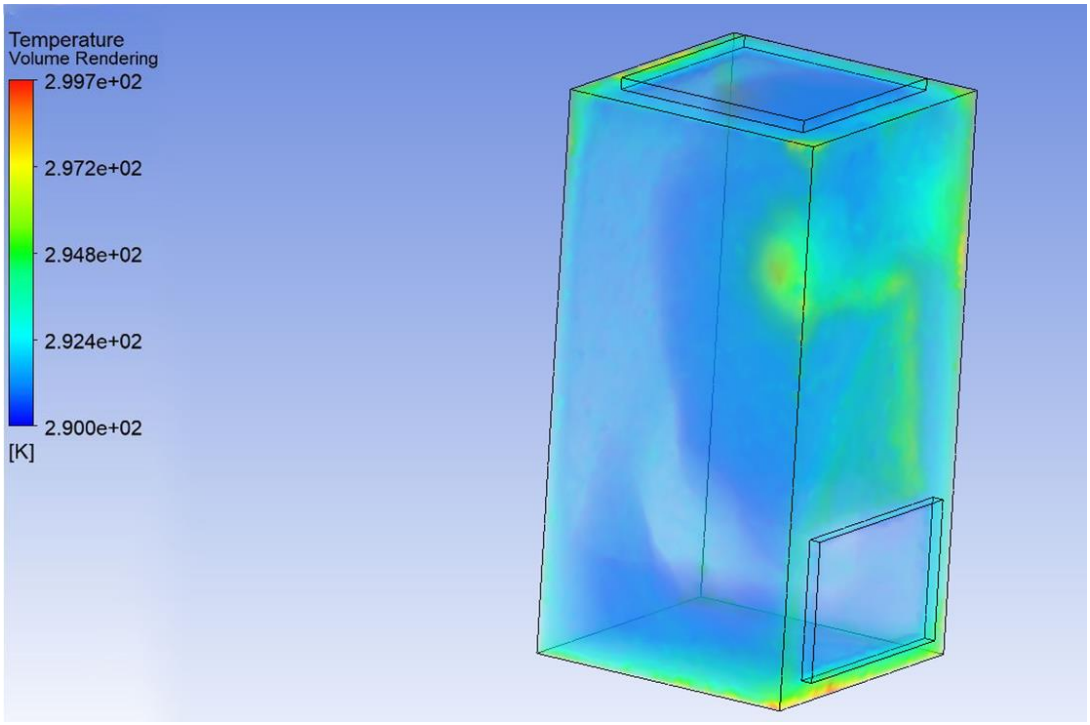

Figure 6. 5: Temperature distribution inside the cold storage.

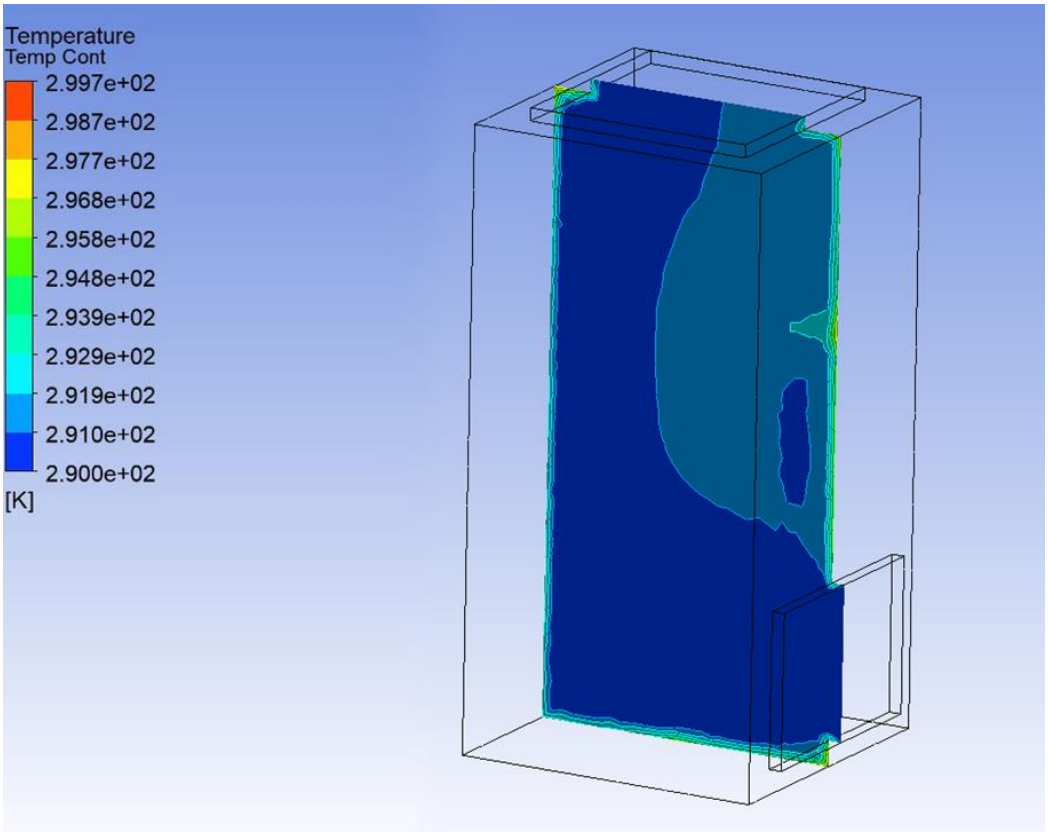

Figure 6. 6: Temperature contour on vertical plane.

6.2. Performance of the cold storage

The effects of the variations of thickness of the cooling pad, velocity and temperature of the air at the inlet on the performance of the evaporative cooler are presented and discussed in this section. Outlet temperature of the air is recorded from the simulation and equations 4.23, 4.25 and 4.26 are used to study the performance of the cooler.

6.2.1. Effect of thickness of pad on outlet temperature

Figure 6.7 show the variation of outlet temperature of the air with the inlet dry bulb temperature of the air at a velocity of 0.5m/s for three different pad thicknesses (50mm, 75mm, 100mm). It is observed that the outlet temperature increases as the inlet air temperature increases but the temperature drop is higher when the inlet temperature is higher and it is lower when the inlet temperature is lower. This is due to the fact that, since the temperature drop is due to evaporation of water from the cooling pad, higher inlet temperatures result in more water to evaporate from the pad and brings more temperature drop in the air. It is also seen that the thickness of the cooling pad has a significant effect on the outlet temperature of the air. As the thickness of the cooling pad increases, the outlet temperature decreases. This is because cooling pads with large thickness can hold more water compared to cooling pads with small thickness. This shows that cooling pads with comparably large thickness are better for evaporative cooling process since lower temperatures are required for cooling. Outlet temperature of 18.91℃ – 23.04℃ at the outlet was also reported by Fayiah-Tumbay et al. (2022).

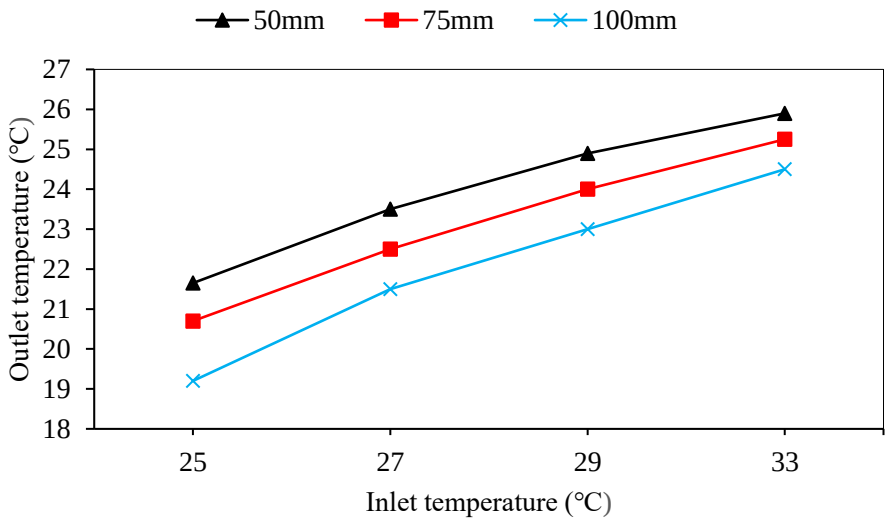

Figure 6. 7: Effect of thickness of cooling pad on outlet temperature at v_{air}=0.5ms.

6.2.2. Effect of thickness of pad on cooling capacity

The variation of cooling capacity of the pad with inlet temperature of the air at inlet velocity of 0.5m/s for three different cooling pad thicknesses (50mm, 75mm, and 100mm) is shown in figure 6.8. The cooling capacity of the pad increases as the inlet temperature of the air increases. As the inlet temperature increases, the rate of water evaporation from the pad increases and this increases the temperature drop of the air which in turn increases the cooling capacity of the pad. The cooling capacity of the pad is also higher for larger thickness of the pad. The cooling pad with 100mm thickness has higher cooling capacity compared to the pad with 75mm thickness which has higher cooling capacity than the pad with 50mm thickness. Increasing the thickness of the pad increases the heat transfer area and, in our case, it increases the rate of water evaporation from the cooling pad to the air. This results in an increase in the temperature drop of the air which increases the cooling capacity. Cooling capacity ranging between 1.384kW and 5.358kW was also reported by Mohammad et al. (2013).

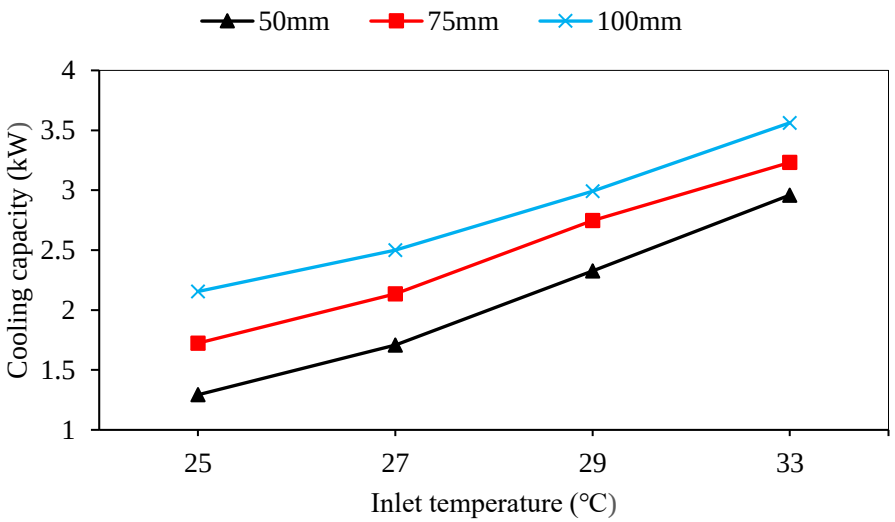

Figure 6. 8: Effect of thickness of cooling pad on cooling capacity at v_a = 0.5m/s.

6.2.3. Effect of thickness of pad on cooling effectiveness

Figure 6.9 show the variation of cooling effectiveness of the pad with the inlet dry bulb temperature of the air at a velocity of 0.5m/s for three different pad thicknesses (50mm, 75mm, 100mm). The cooling effectiveness also known as pad effectiveness depends on the temperature difference of

the air between the inlet and outlet of the cooling pad. The cooling effectiveness is higher when there is larger temperature difference and it decreases when the temperature difference decreases. From figure 6.7 we have seen that the cooling pad with 100mm thickness has the lowest outlet temperature compared to the cooling pad with 75mm and 50mm thickness and the outlet temperature of the cooling pad with 75mm thickness is lower than the pad with 50mm thickness. Therefore, the colling pad with 100mm thickness has higher temperature drop of air than the cooling pad with 75mm thickness which has higher temperature drop than the cooling pad with 50mm thickness. Due to this, the effectiveness of the pad increases as its thickness increases as shown in figure 6.9. It is also observed that the effectiveness of the cooling pad increases as the inlet temperature of the air increases. This is also related to the temperature drop of the air since the temperature drop is higher when the inlet temperature is high and decreases when the inlet temperature decreases. The average effectiveness was 84.77% and Zakari et al. (2016) and Babaremu et al (2018) reported cooling efficiency of 83% and 86.01% respectively.

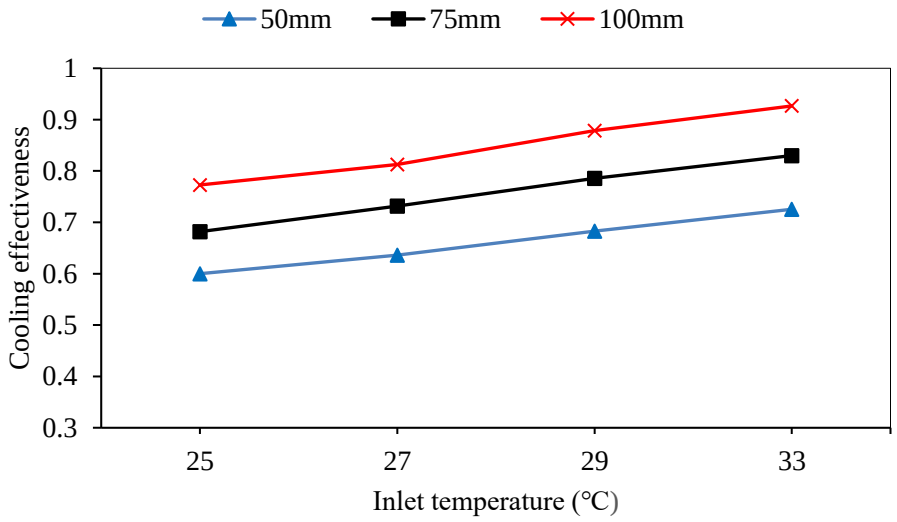

Figure 6. 9: Effect of thickness of cooling pad on cooling effectiveness at v_a = 0.5m/s.

6.2.4. Effect of inlet velocity on outlet temperature at different thickness of pad

Variation of outlet air temperature with respect to velocity of the air at three different pad thickness (50mm, 75mm, 100mm) is shown in figure 6.10 (a-d). Figure 6. 10 (a) shows the outlet temperature at an ambient temperature of 25°C, Figure 6.10 (b) shows the outlet temperature when the ambient temperature is 27°C, Figure 6.10 (c) shows the outlet temperature when the ambient temperature

is 29℃ and Figure 6.10 (d) shows the outlet temperature when the ambient temperature is 33℃. From these figures it is observed that as the velocity of the air increases, the outlet temperature also increases. The required cooling conditions are achieved at lower velocity of air. The result also shows that the outlet temperature is lower at the lowest inlet temperature (25℃, figure 6.10 (a)) and increases as the inlet temperature increases. For each case, as the thickness of the cooling pad increase, the outlet temperature decreases. The lowest outlet temperature achieved is 19.2℃ when the inlet velocity is 0.5m/s, inlet temperature is 25℃ and the thickness of the cooling pad is 100mm. For all cases considered, the lowest outlet temperature was achieved when the inlet velocity is 0.5m/s and the thickness of the pad is 100mm.

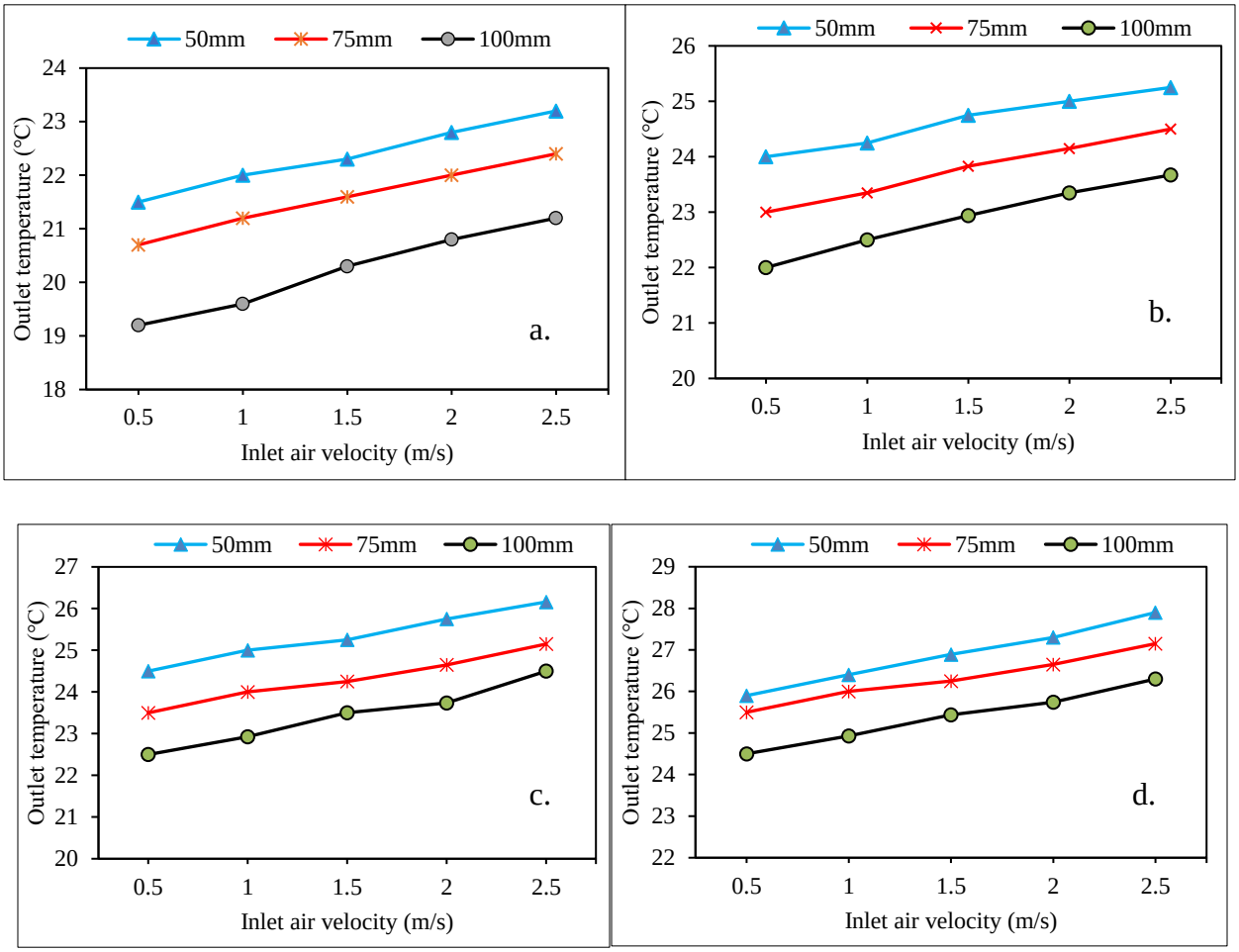

Figure 6. 10: Effect of inlet velocity of air on outlet temperature at different thickness of pad and at inlet temperature of a) at 25℃, b) 27℃, c) 29℃ and d) 33℃.

6.2.5. Effect of inlet velocity on cooling capacity at different thickness of pad

Cooling capacity of the evaporative cooler variation with velocity of the air at three different pad thicknesses (50mm, 75mm, 100mm) is shown in figure 6.11 (a-d). Figure 6.11 (a) shows the cooling capacity at an ambient temperature of 25℃, Figure 6.11 (b) shows the cooling capacity at an ambient temperature of 27℃, Figure 6.11 (c) shows the cooling capacity when the ambient temperature is 29℃ and Figure 6.11 (d) shows the cooling capacity when the ambient temperature is 33℃. The results shows that the cooling capacity increases as both the inlet air velocity and thickness of cooling pad increases. This is due to the fact that increasing velocity of the air means increasing the air flow which in turn increases the cooling capacity and increasing the thickness of the pad means increasing the heat transfer area which also increases the cooling capacity. The cooling capacity also increases as the inlet temperature of the air increases since the temperature drop is higher at higher inlet temperatures. In each case, the cooling capacity is high at the highest inlet velocity (2.5m/s) and at the largest pad thickness (100mm).

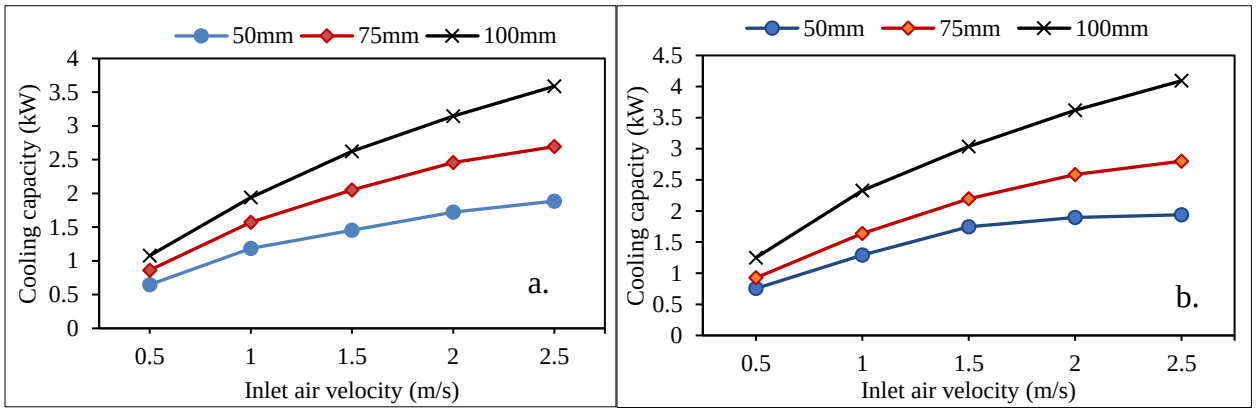

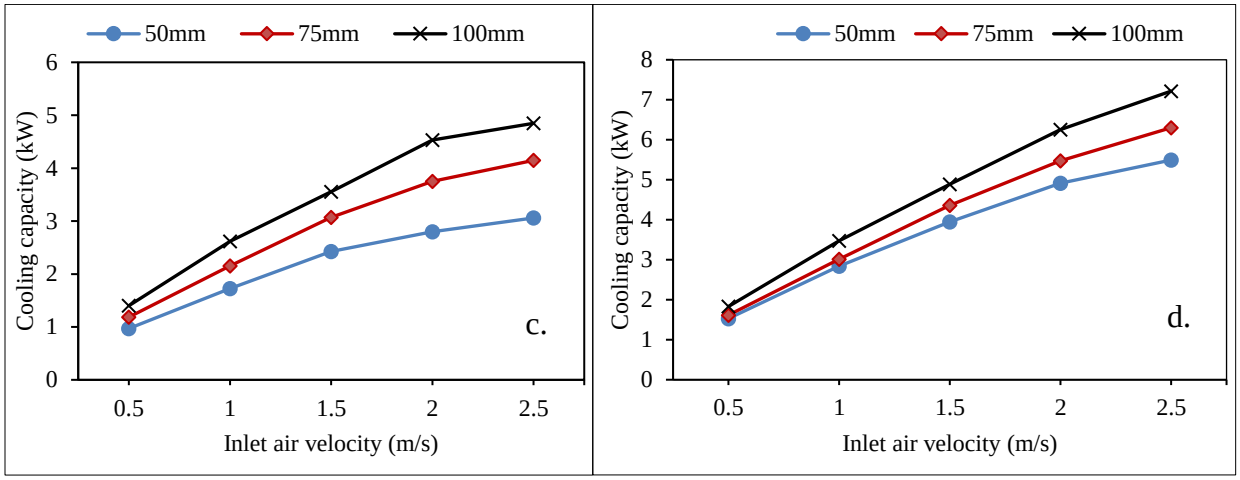

Figure 6. 11: Effect of inlet velocity of air on cooling capacity at different thickness of pad and at inlet temperature of a) at 25℃, b) 27℃, c) 29℃ and d) 33℃.

6.2.6. Effect of inlet velocity on cooling effectiveness at different thickness of pad

Figure 6.12 (a-d) shows the variation of cooling effectiveness of the evaporative cooler with respect to velocity of the air at three different pad thicknesses (50mm, 75mm, 100mm). Figure 6.12 (a) shows the cooling effectiveness at an ambient temperature of 25℃, Figure 6.12 (b) shows the cooling effectiveness when the ambient temperature is 27℃, Figure 6.12 (c) shows the cooling effectiveness when the ambient temperature is 29℃ and Figure 6.12 (d) shows the cooling effectiveness when the ambient temperature is 33℃. The cooling effectiveness also known as pad effectiveness depends on the temperature difference of the air between the inlet and outlet of the cooling pad where larger temperature differences results in high effectiveness. From the result it is seen that the effectiveness of the cooling pad is higher when the thickness of the pad is large whereas the pad effectiveness decreases when the inlet velocity of the air increases. This is due to the fact that large pad thickness increases the heat transfer area which in turn increases the temperature drop between the inlet and the outlet. Increasing the inlet velocity decreases the residence time of the air in the cooling pad which decreases the temperature drop of the air. Thus, increasing the thickness of the cooling pad increases the effectiveness of the pad and increasing the velocity of the air decreases the effectiveness of the pad. High cooling effectiveness is achieved at the larger cooling pad thickness and low inlet velocity of the air. Results with similar trends of cooling effectiveness are also reported by Olosunde et al. (2016).

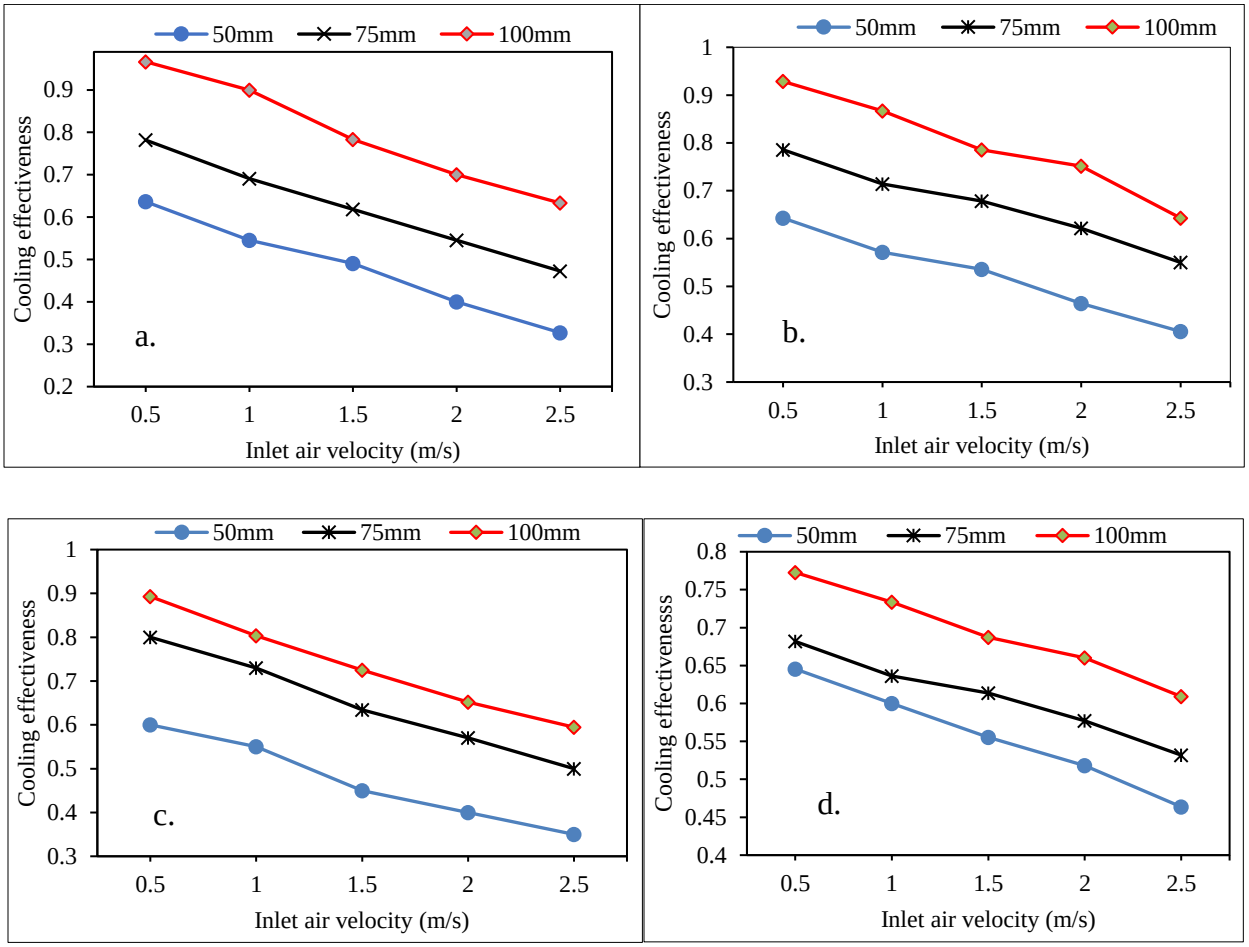

Figure 6. 12: Effect of inlet velocity of air on cooling effectiveness of the pad at different thickness of pad and at inlet temperature of a) at 25℃, b) 27℃, c) 29℃ and d) 33℃.

6.2.7. Effect of inlet velocity on COP at different thickness of pad

Figure 6.13 (a-d) shows the variation of COP of the evaporative cooler with respect to velocity of the air at three different pad thicknesses (50mm, 75mm, 100mm). Figure 6.13 (a) shows the COP variation at an ambient temperature of 25℃, Figure 6.13 (b) shows the COP when the ambient temperature is 27℃, Figure 6.13 (c) shows the COP when the ambient temperature is 29℃ and Figure 6.13 (d) shows the COP when the ambient temperature is 33℃. As expressed in equation 4.26, the COP is related to the cooling capacity of the evaporative cooler. As the cooling capacity of the evaporative cooler increases, its coefficient of performance also increases. Therefore, the increase in thickness of the cooling pad and increase in inlet velocity of the air increases the COP.

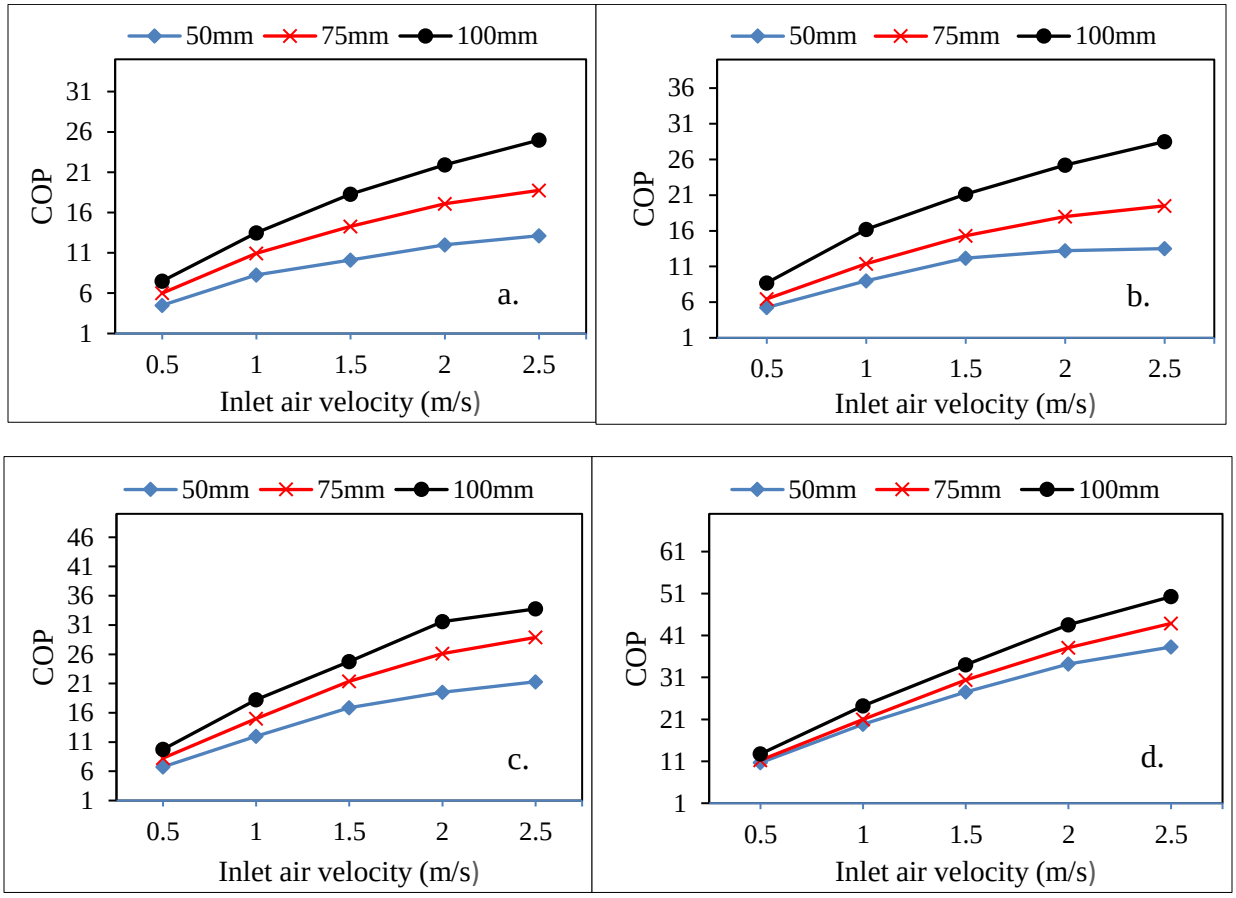

Figure 6. 13: Effect of inlet velocity of air on COP at different thickness of pad and at inlet temperature of a) at 25℃, b) 27℃, c) 29℃ and d) 33℃.

CHAPTER SEVEN

7. CONCLUSION AND RECOMMENDATION

7.1. Conclusion

Kombolcha is one of the large tomatoes producing regions in Ethiopia. But due to its semi-arid climate condition and low electric power coverage 20% of the produced tomatoes gets spoiled. Tomatoes do not require a very low temperature for storage like other vegetables. Their storage temperature is between 18℃ to 22℃. Therefore, the evaporative cooler can be a best solution for proper storage of tomato. Evaporative cooling system consumes a small amount of power to maintain the required storage temperature for the specified amount of tomato when compared to normal refrigeration system. A direct evaporative cooler is designed to store 100kg tomato and its performance is studied with simulation with ANSYS Fluent simulation software. The pump and fan required for the evaporative cooling system are of small capacity with a power consumption of 5w and 9.36w, respectively. The effects of parameters like thickness of the cooling pad, inlet velocity of the air, and inlet ambient dry bulb temperature on the performance of the evaporative cooler is studied. The result of the simulation shows that, the temperature drops of the air between the inlet and the outlet of the cooler increase as the thickness of the cooling pad and the inlet velocity of the air increase. The cooling effectiveness of the pad also increases as the thickness of the pad increases but it decreases as the velocity of the air increases. The cooling capacity of the pad and COP increases when the thickness of the pad and the inlet velocity of the air increases.

7.2. Recommendation

The solar powered evaporative cooler for tomato storage is a simple and light apparatus with different parts. But kombolcha is not only known for its tomato products. Thus, to make the design more flexible and friendlier, I recommend the following points for further research. Adopting the solar powered evaporative cooler for other agricultural products as well and making the whole system mobile in order to cool the product until it reaches the market. Experimental study to validate the results of the simulation is also recommended.

REFERENCES

ADEBISI, W. (2015). DEVELOPMENT OF A SOLAR POWERED EVAPORATIVE COOLING STORAGE SYSTEM FOR TROPICAL FRUITS AND VEGETABLES. *Food Processing and Preservation* 1745-4549 https://doi.org/10.1111/jfpp.12605

Akdanye. (2019). Quality Changes in Apple in Evaporative Cooling Store. https://doi.org/10.1007/s10341-019-00458-w

Akdemir, S., & Bal, E. (2020). Quality changes in apple in evaporative cooling store. *Erwerbs-Obstbau*, *62*(1), 61-67.

Ambuko, J., & Wanjiru, F. (2017). Preservation of Postharvest Quality of Leafy Amaranth (Amaranthus spp.) Vegetables Using Evaporative Cooling. *Journal of Food Quality*, *2017*, 5303156. https://doi.org/10.1155/2017/5303156

Amjad. (2021). Solar-Hybrid Cold Energy Storage System Coupled with Cooling Pads Backup: A Step towards Decentralized Storage of Perishables. *Energies*, 2-20. https://doi.org/10.3390/en14227633

Arputham, D. (2021). Design and Performance of Solar PV Integrated Domestic Vapor Absorption Refrigeration System. *International Journal of Photoenergy*, *2021*, 6655113. https://doi.org/10.1155/2021/6655113

Ayele, L. (2018a). Designing and experimental testing of solar powered evaporative cooling to store perishable agricultural products. 18-100.

Ayele, L. (2018b). Designing and experimental testing of solar powered evaporative cooling to store perishable agricultural products.

Ayele, L. (2020). *Designing and experimental testing of solar powered evaporative cooling to store perishable agricultural products*

Babaremu. (2018). DESIGN AND OPTIMIZATION OF AN ACTIVE EVAPORATIVE COOLING SYSTEM. *Mechanical Engineering and Technology (IJMET)*, *9*(10), 1051-1061.

Basediya, A. l., Samuel, D. V. K., & Beera, V. (2011). Evaporative cooling system for storage of fruits and vegetables - a review. *Food Scientists & Technologists*, *50*(3), 429–442. https://doi.org/10.1007/s13197-011-0311-6

Beera, A. B. D. V. K. S. V. (2013). Evaporative cooling system for storage of fruits

and vegetables. *J Food Sci Technol*, *50*(3), 429-422.

Bhatia, A. (2001). Cooling load calculations and principles. *Continuing Education and Development, Inc. New York*, *877*, 39.

Branthôme, F.-X. (2022). *Worldwide (total fresh) tomato production*. https://www.tomatonews.com/en/worldwide-total-fresh-tomato-production-exceeds-187-million-tonnes-in-2020_2_1565.html

Chaudhari, B. D., Sonawane, T. R., Patil, S. M., & Dube, P. A. (2015). A Review on Evaporative Cooling Technology. *International Journal of Research in Advent Technology*, *3*(2).

Deshmukh, G., Birwal, P., Datir, R., & Patel, S. (2017). Thermal Insulation Materials: A Tool for Energy Conservation. *Journal of Food Processing & Technology*, *08*(04). https://doi.org/10.4172/2157-7110.1000670

Ekpunobi, U. E., Ukatu, S. C., Ngene, B. O., Onyema, C. T., & Ofora, P. U. (2014). Investigation of the thermal properties of selected fruits and vegetables.

Gross, K. C., Wang, C. Y., & Saltveit, M. E. (2016). *The commercial storage of fruits, vegetables, and florist and nursery stocks*. United States Department of Agriculture, Agricultural Research Service ….

H. Getinet, T. S., K. Woldetsadik. (2008). The effect of cultivar, maturity stage and storage environment on quality of tomatoes. *Food Engineering* 467–478. https://doi.org/10.1016/j.jfoodeng.2007.12.031

IIT Kharagpur. (2008). *4O LESSONS ON REFRIGERATION AND AIR CONDITIONING* (Vol. 1). Department of Electrical Engineering.

Islam, M. P. (2014). A new zero energy cool

chamber with a solar-driven adsorption refrigerato. *Solar adsorption system*, 367–376. https://doi.org/10.13140/RG.2.1.3556.2006

J.K.Jain, & D.A.Hindoliya. (2011). Experimental performance of new evaporative cooling pad materials. *Sustainable Cities and Society*, *1*(4), 252-256.

J.T. Libertya*, B. O. U., S.A Pukumab and C.E Odoc. (August 2013). Principles and Application of Evaporative Cooling Systems for Fruits and Vegetables Preservation. *Vol.3*(No.3).

Jain, D. (2007). Development and testing of two-stage evaporative cooler. *Building and Environment*, *42*(7), 2549-2554. https://doi.org/10.1016/j.buildenv.2006.07.034

Jitendra Jayant, A. S. (2016). COOLING LOAD CALCULATION FOR A POTATO COLD STORAGE PLANT. *International Journal of Innovative Research in Engineering & Science*, *3*(5).

Kenghe, R. (2015). Design, development and performance evaluation of an on-farm evaporative cooler. *International Journal of Science, Technology and Society*, *3*(2-2), 1-5.

Kesavan, M. (2018). Performance Evaluation of Evaporative Cooler using Luffa Fiber Materials. *International Journal of Engineering Research & Technology*, *7*(9).

Khakre, V., Wankhade, A., & Ali, M. (2017). Cooling load estimation by CLTD method and hap 4.5 for an evaporative cooling system. *Int. Res. J. Eng. Technol*, *4*(1), 1457-1460.

Khan, F. A., Bhat, S. A., & Narayan, S. (2017). Storage methods for fruits and vegetables. *Sher-e-Kashmir University of Agricultural Sciences and Technology of Kashmir. Shalimar*.

Kraemer, R., Plouff, A., & Venn, J. (2015). Design of a Small-Scale, Low-Cost Cold Storage System. *Robert Kraemer, Andrew Plouff, John Venn*, *B*(487).

Kulkarni, R., & Rajput, S. (2013). Comparative performance analysis of evaporative cooling pads of alternative configurations and materials. *International Journal of Advances in Engineering & Technology*, *6*(4), 1524.

Lizcano, D. C., Rocha, J. G.-D., & Kleit, M. (2020). *Direct Evaporative Cooling System for Tomatoes in India* McGill University].

Mahmood, M. H., Sulta, M., & Miyazaki, T. (2019). Solid desiccant dehumidification-based air-conditioning system for agricultural storage application: Theory and experiments. *Journal of power and energy*, *0*(0), 1-14. https://doi.org/10.1177/0957650919869503

Muhammad, N. J. (2016). DESIGN AND CONSTRUCTION OF AN EVAPORATIVE COOLING SYSTEM FOR THE STORAGE OF FRESH TOMATO. *Engineering and Applied Sciences*, 2340-2348.

Ndukwu, M., Ibeh, M. I., Akpan, G. E., Ugwu, E., Akuwueke, L., Oriaku, L., Ihediwa, V. E., Abam, F. I., Wu, H., & Kalu, C. (2023). Analysis of the influence of outdoor surface heat flux on the inlet water and the exhaust air temperature of the wetting pad of a direct evaporative cooling system. *Applied Thermal Engineering*, *226*, 120292.

Ndukwu, M., Manuwa, S., Olukunle, O., & Oluwalana, I. (2013). Mathematical model for direct evaporative space cooling systems. *Nigerian Journal of Technology*, *32*(3), 403-409.

Peter Ross Enterprises. (2019). *Direct Evaporative Coolers vs. Indirect Evaporative Coolers: What are Their Differences?* https://evaporative-coolers.com.au

Putter, H. d., Hengsdijk, H., Roba, S. T., & Wayu, D. A. (2012). *Scoping study of horticulture smallholder production in the Central Rift Valley of Ethiopia* (Plant Research International, Issue.

R. A. Bucklin, J. D. L., D. B. McConnell, and E. G. Wilkerson. (2016). Fan and Pad Greenhouse Evaporative Cooling Systems.

ROLLINGS, T. (2019). *DESIGN, CONSTRUCTION AND TESTING OF AN IMPROVED SOLAR POWERED EVAPORATIVE COOLING SYSTEM* MAKERERE UNIVERSITY].

Samue, A. l. B. D. V. K. (2013). Evaporative cooling system for storage of fruits and vegetables. *Food Scientists & Technologists*, *50*(3), 429-423. https://doi.org/10.1007/s13197-011-0311-6

Shahzad, M. W. (2019). An improved indirect evaporative cooler experimental investigation. *Applied Energy*. https://doi.org/10.1016/j.apenergy.2019.113934

Sibanda, S. (2019). *DEVELOPMENT OF A SOLAR POWERED INDIRECT AIR COOLING COMBINED WITH DIRECT EVAPORATIVE COOLING SYSTEM FOR STORAGE OF FRUITS AND VEGETABLES IN SUB-SAHARAN AFRICA* KwaZulu-Natal]. Pietermaritzburg, South Africa.

Sibanda, S. (2020). Potential causes of postharvest losses, low-cost cooling technology for fresh produce farmers in SubSahara Africa. *African Journal of Agricultural Research*, *16*(5), 553-566. https://doi.org/10.5897/AJAR2020.14714

Sibanda, S., & Workneh, T. S. (2020). Performance evaluation of an indirect air cooling system combined with evaporative cooling. *Heliyon*, *6*(1), e 03286. https://doi.org/10.1016/j.heliyon.2020.e03286

Sibanda, S., & Workneh, T. S. (2020). Potential causes of postharvest losses, low-cost cooling technology for fresh produce farmers in Sub-Sahara Africa. *African Journal of Agricultural Research*, *16*(5), 553-566.

Soh, G. Y., Yeoh, G. H., & Timchenko, V. (2016). An algorithm to calculate interfacial area for multiphase mass transfer through the volume-of-fluid method. *International Journal of Heat and Mass Transfer*, *100*, 573-581.

Tamrat, B., Ayele, L., & Kathiravan, R. (2021). Design and Experimental Test on Solar Powered Evaporative Cooling to Store Perishable Agricultural Products. Advances of Science and Technology: 8th EAI International Conference, ICAST 2020, Bahir Dar, Ethiopia, October 2-4, 2020, Proceedings, Part II 8,

Tasobya, R. (2019). *Design, construction and testing of an improved solar powered evaporative cooling system* Makerere University].

Taye S. Mogaji, a. O. P. F. (2011). Development of an evaporative cooling system for the preservation of fresh vegetables. *African Journal of Food Science*, *5*(4).

Tegegn, A. (2013). *VALUE CHAIN ANALYSIS OF VEGETABLES: THE CASE OF HABRO AND KOMBOLCHA WOREDAS IN OROMIA REGION, ETHIOPIA* Haramaya University].

Tesema, S., & Bekele, G. (2015). Resource assessment and optimization study of efficient type hybrid power system for electrification of Rural District in Ethiopia. *International Journal of Energy and Power Engineering*, *3*(6), 331-334. https://doi.org/10.11648/j.ijepe.20140306.1

Timothy. (2019). Evaluation of an active evaporative cooling device for storage of fruits and vegetables. *Agricultural and Biosystems Engineering 21*(1), 1256-1261.

Tolesa, G. N., & Workneh, T. S. (2017). Influence of storage environment, maturity stage and pre-storage disinfection treatments on tomato fruit quality during winter in KwaZulu-Natal, South Africa. *journal of food science and technology*, *54*, 3230-3242.

Vanndy. (2008). Evaporative Cooling Storage of Tomato in Cambodia and Laos. *Agronomy and Agricultural Land*

565-570.

Verploegen, E., Ekka, R., & Gill, G. (2019). *EVAPORATIVE COOLING FOR IMPROVED FRUIT & VEGETABLE STORAGE IN RWANDA & BURKINA FASO*.

Workneh, S. S. a. T. S. (2020). Determination of solar energy requirements for indirect

cooling combined with evaporative cooling for storage of fresh produce. *Agricultural Research*, *16*(10), 1420-1431. https://doi.org/10.5897/AJAR2020.15098

Zakari, M., Abubakar, Y., Muhammad, Y., Shanono, N., Nasidi, N., Abubakar, M., Muhammad, A., Lawan, I., & Ahmad, R. (2016). Design and construction of an evaporative cooling system for the storage of fresh tomato. *ARPN Journal of Engineering and Applied Sciences*, *11*(4), 2340-2348.

Zakari M. D, Y. S. A., Muhammad, Y. B., Shanono, N. J., Nasidi, N. M., Abubakar, M. S., Muhammad, A. I., Lawan, I., & Ahmad, R. K. (2016). DESIGN AND CONSTRUCTION OF AN EVAPORATIVE COOLING SYSTEM FOR THE STORAGE OF FRESH TOMATO. *Journal of Engineering and Applied Sciences*, *11*(4). https://doi.org/10.13140/RG.2.1.4748.4569